AN ABSTRACT OF THE THESIS OF

Joshua L. Snider for the degree of Honors Baccalaureate of Science in Bioengineering presented on May 17, 2013. Title: Characterization and application of PEO-containing triblock copolymer surfactants.

Abstract approved:

_____

Joseph McGuire

The action of pendant, polyethylene oxide (PEO) brush layers as nonfouling coatings for biomedical materials is well understood. However progress toward clinical application of stable, high density PEO coatings has historically been impeded by the lack of cost effective, non-invasive methods for their preparation. Triblock polymers featuring a hydrophobic, polypropylene oxide (PPO) or polybutadiene (PB) centerblock flanked by two PEO side chains can be used to coat the surfaces of hydrophobic biomedical materials, and in this way render them less prone to protein adsorption and bacterial adhesion. Optimal coating requires awarenesss of triblock aggregation properties, and for this purpose pyrene fluorescence quenching was used to determine the critical aggregation concentration of the triblocks used in this work. Coatings produced by radiolytic grafting of PEO-PB-PEO triblocks to polyacrylonitrile membranes used in hemodialysis were evaluated in relation to impact on urea permeability through the membrane. Neither the PEO-PBD-PEO triblocks nor the irradiation process was observed to have any effect on membrane permeability to urea. Beyond issues surrounding biocompatibility, PEO coatings can potentially be used to entrap and later release bioactive

peptides for short-term medical device applications. In this context pyrene fluorescence quenching was used to determine the existence of a hydrophobic inner region of PEO layers based on PEO-PPO-PEO triblocks, substantially explaining the high affinity for entrapment previously recorded for amphiphilic peptides.

Key Words: biocompatibility, PEO-PBD-PEO, brush layer

Corresponding E-mail Address: snidejos@onid.orst.edu

© Copyright by Joshua L. Snider

May 17, 2013

All Rights Reserved

Characterization and application of PEO-containing triblock copolymer surfactants

by

Joshua L. Snider

A PROJECT

submitted to

Oregon State University

University Honors College

in partial fulfillment of

the requirements for the

degree of

Honors Baccalaureate of Science in Bioengineering (Honors Scholar)

Presented May 17, 2013

Commencement June 2013

Honors Baccalaureate of Science in Bioengineering project of Joshua L. Snider presented on May 17, 2013.

APPROVED:

_____

Mentor

_____

Committee Member

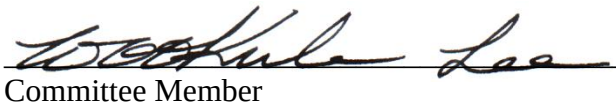

_____

Committee Member

_____

Head, Department of Chemical, Biological & Environmental Engineering

_____

Dean, University Honors College

I understand that my project will become part of the permanent collection of Oregon State University, University Honors College. My signature below authorizes release of my project to any reader upon request.

_____

Joshua L. Snider, Author

ACKNOWLEDGEMENTS

I would like to thank my mentor, Dr. Joseph McGuire, Dr. Karl Schilke, and Dr. Phil Harding for all of their valuable guidance through all stages of the research and reporting process. I would also like to thank Dr. Woo-Kul Lee for his leadership and guidance on the urea transport section of research and for being a part of my thesis committee. A special thanks to Rose Felber and Lauren Jansen for their help in the lab for the urea transport and CAC experiments, respectively. Keely Heintz and Mitchell Truong also deserve great thanks for their work designing the b-galactosidase tests for protein repulsion analysis. I would also like to thank Dr. Angelicque White and Katie Watkins-Brandt for allowing me to use their fluorometer for the CAC and hydrophobic layer analyses. I would like to thank the OSU Department of Chemical, Biological, and Environmental Engineering and its faculty for providing both equipment and guidance where I needed it during research. Finally, I would like to thank my friends and family for supporting me through all of my research.

CONTRIBUTION OF AUTHORS

My research mentor, Dr. Joseph McGuire, as well as Dr. Karl Schilke, assisted in the editing of this paper and in the formulation of the abstract. Rose Felber and Lauren Jansen assisted with much of the experimentation for the urea transport and CAC determination projects, respectively.

TABLE OF CONTENTS

LIST OF FIGURES

LIST OF TABLES

LIST OF APPENDICES

1 INTRODUCTION

1.1 Protein adsorption on surfaces

Biocompatibility of medical devices is a large issue in the medical industry. Protein adsorption to devices is prominent due to the fact that many processes deal with contact between bodily fluids (i.e. blood) and hydrophobic surfaces. When proteins contact hydrophobic surfaces, such as those of many plastics used in medical devices, they adsorb to the surface and cause unwanted events to occur, including coagulation and membrane fouling.

The current standard procedure used to minimize the occurrence of these unwanted events is the administration of blood thinners to patients. However, this procedure carries other issues with it. Patients on blood thinners must be monitored very closely to avoid out-of-control bleeding. In addition, regular patients, such as those on hemodialysis that come in multiple times a week for treatment, could end up paying substantial amounts of money for blood thinners.

1.2 Triblock surfactants

It has been shown in recent studies that biocompatibility of surfaces can be greatly improved by coating a surface with polyethylene oxide (PEO) chains (Lee, Martin, and Tan 1989). Adsorption of enough PEO chains allows for the creating of a "brush layer", which serves as a barrier between incoming proteins and the surface. The creation of copolymers of PEO has only helped the ability to effectively "cloak" a surface from proteins. One group of these copolymers that is widely used in surface coatings is known as Pluronic® copolymers. This group is made up of so-called

triblock copolymers because of their inclusion of three blocks: two PEO chains linked by a polypropylene (PPO) centerblock, as seen in Figure 1.1.

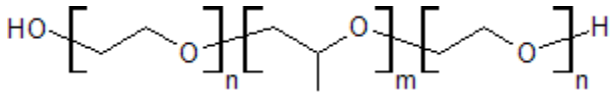

Figure 1.1: *Basic structure of Pluronic® copolymers. The letters n and m refer to the lengths of the PEO and PPO chains, respectively.*

The PPO centerblock allows for the Pluronic® to adsorb to hydrophobic surfaces and leave the PEO chains to extend out from the surface. Adsorption of enough triblocks to a surface allows for brush layer formation, just as with the PEO chains alone. These triblocks can also be covalently bonded to a surface through silanization of a surface, followed by γ-irradiation, as discussed in McPherson et al. and shown in Figure 1.2 (McPherson, Shim, and Park 1997).

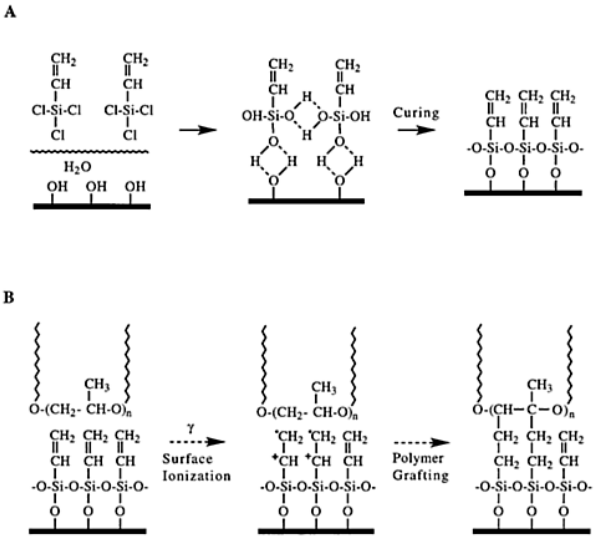

Figure 9. Schematic representation of (A) surface silanization by TCVS and (B) proposed mechanism of covalent grafting of Pluronics® to the TCVS-primed surface.

Figure 1.2: *Basic schematic from McPherson, et al. showing the process of covalent grafting of Pluronics® to TCVS-treated surfaces (McPherson et al. 1997).*

A novel triblock copolymer has been developed by Dr. Marc Hillmeyer at the University of Minnesota. The structure replaces the PPO of the Pluronics® with a polybutadiene (PBD) chain as a centerblock. This new centerblock allows for covalent grafting of these triblocks to untreated polymer surfaces with γ-irradiation, due to the presence of vinyl groups in PBD.

A special set of triblock copolymers were designed by Dr. Karl Schilke. These triblocks are very similar to the Hillmeyer triblocks in chain configuration, but they carry a significant difference: the PEO chains are cleavable from the PBD centerblocks. Cleavage of the PEO chains would allow for visualization of the arrangement of the adsorbed triblocks. Six different types of cleavable triblocks were made and are referred to as CT121, CT131, CT222, CT232, CT525, and CT535 for the approximate sizes, in kDa, of the PEO and PBD chains (the first and third numbers referring to the PEO chains, and the second number referring to the PBD chain).

2 PROCEDURES AND METHOD

2.1 *Membrane permeability*

Medical devices, such as hemodialysis devices, would be coated with triblock copolymer to impart biocompatibility, so the possible effects of the coating on transport through the membrane must be explored. To investigate this, a flow cell was designed to examine urea transport from one cell to another across a membrane. The flow cell was composed of two 80-mL compartments separated by a membrane and sealed with PVC gaskets, leaving 16 cm^2 of membrane exposed for transport. One

compartment was connected to a 320-mL beaker via Tygon tubing and pumps to effectively increase the volume of the compartment. Two Masterflex L/S pumps were used to circulate the PBS through the one compartment to the beaker. The flow rate of the pump pulling from the 320-mL beaker was set to 120 mL/min, while that of the pump pulling from the 80-mL compartment was set to 165 mL/min. The tubing was set up in such a way to allow the 80-mL compartment to fill to 80 mL but not overflow due to the higher pumping rate from the one pump. This 400-mL compartment was designed to be the sink for the urea (deemed the "reservoir"), while the smaller compartment (deemed the "urea compartment") was designed to be the source of urea in order to promote maximum urea transport. A schematic of the flow cell can be seen in Figure 2.1.

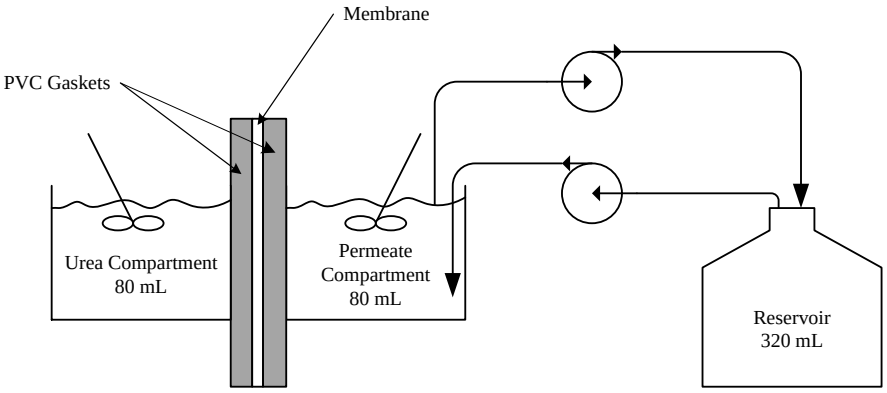

Figure 2.1: *Basic schematic of flow cell for urea transport tests.*

AN69 and AN69-ST polyacrylonitrile membranes (Gambro, Lund, Sweden) were used for the membrane permeability tests. The two membranes are identical except that the AN69-ST includes a coating of polyethylenimine (PEI) to mask the

net negative charge of the membrane surface. Four-inch squares were cut from this membrane to fit the flow cell.

Coating of the membranes with triblocks was carried out by placing the membranes into a device designed to contact one side of the membrane (the PEI-coated side for the AN69-ST) with a 5 mg/mL solution of triblocks (see Figure 2.2 for picture of device). Triblock solution was injected into the device via slits in the top (about 5 mL in each compartment) and the entire device was subjected to 0.8 MRad of radiation to covalently bond the triblocks.

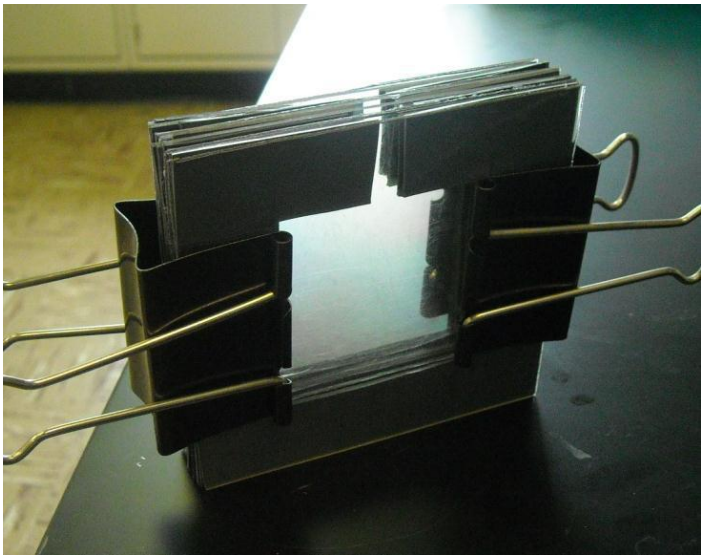

Figure 2.2: *Photo of device used to hold membrane pieces during irradiation. Polycarbonate sheets and gaskets were used to separate membrane sheets and allow contact of triblocks with only one side of the membrane. Twenty five square centimeters of each membrane were allowed to contact the triblock solution.*

Solutions of urea were made by adding 0.3 mg/mL urea (Fisher Scientific, Hampton, NH) to 10 mM, pH 7.4 phosphate buffered saline (PBS). Membrane sheets were loaded such that, if coated, the triblock-coated side of the membrane contacted

the urea solution. If uncoated, the PEI-coated side of the membrane contacted the urea solution (AN69-ST only).

Each test was started with the simultaneous addition of 80 mL urea in PBS to the urea chamber, 80 mL of PBS to the reservoir chamber, and 320 mL of PBS to the reservoir beaker. The electric mixers were started, along with the reservoir pumps, and initial 200-μL samples were taken and stored in microcentrifuge tubes at 4 °C. Samples were continually taken every 30 minutes over a total testing time of 5 hours. Some tests included the addition of bovine serum albumin (BSA), fibrinogen, or lysozyme to test for the ability of the membrane (triblock coated and bare) to repel proteins.

The concentrations of the urea were determined using a urea assay first developed by Jung et al. and later improved by Zawada et al. The two reagents for the assay (deemed the *o*-phthalaldehyde reagent and the primaquine bisphosphate reagent) were made and stored separately at 4 °C. After testing, 50 μL of each sample was added to a different well of a 96-well plate along with 100 μL of each reagent (total well volume of 250 μL). Solutions for standard curve generation were also created and tested in the same fashion and alongside the experimental samples. Jung et al. used solutions containing 5, 4, 3, 2, 1, and 0 mg/dL urea to create a standard curve; however, it was deduced by Zawada et al. that the 5 and 0 mg/dL solutions were sufficient to create a standard curve. (Jung, Biggs, Erikson, and Ledyard 1975; Zawada, Kwan, Olszewski, Llinas, and Huang 2009)

The well plate was then incubated at 35 °C for one hour to maintain constant reaction temp. Following incubation, light absorbance of the samples at 450 nm was

measured using a PerkinElmer 1420 Multilabel Counter VICTOR^{3}V photospectrometer (PerkinElmer, Waltham, MA).

2.2 *Critical aggregation concentration (CAC)*

Surfactants are known to aggregate in solution due to their amphiphilic nature. The concentration at which these aggregates are formed is known as the critical aggregation concentration (CAC). For example, triblock copolymer surfactants form aggregates above their CACs in which the hydrophobic centerblocks are pointing inwards toward one another and the hydrophilic chains are extending out into solution (as seen on the right-hand side of Figure 2.2). The CAC is a characteristic that can help understand surfactant behavior in solution and is known for many industrially-used surfactants. However, the values of CACs for many surfactants can vary drastically in literature.

A method called fluorescence quenching is one way to determine the CAC of a surfactant. Some fluorescent molecules are known to be quenched in certain environments. For example, the fluorescence of pyrene is known to be quenched in hydrophobic environments such as those created by the aggregation of surfactants. The fluorescence quenching method utilizes this phenomenon to determine the CAC of surfactants. Pyrene was chosen for this study, because it is highly sensitive to the hydrophobicity of its environment and is commonly used in CAC determination tests. The excitation wavelength of pyrene varies depending on the source, so initial testing was done to find an optimal wavelength. The emission peaks for pyrene fall around 370 and 395 nm; optimization of this wavelength was also done in the initial testing phase.

Plotting fluorescence intensity at the emission peak versus the log of the surfactant concentration will give two distinct linear regions in the data, given that the data circumvents the CAC (see Figure 2.3). At the CAC of the surfactant, there will be a significant increase in the slope of the data due to the increase in fluorescence brought about by the formation of aggregates. The point at which this spike in intensity occurs (or where the two linear regions intersect) is known to be the CAC of the surfactant.

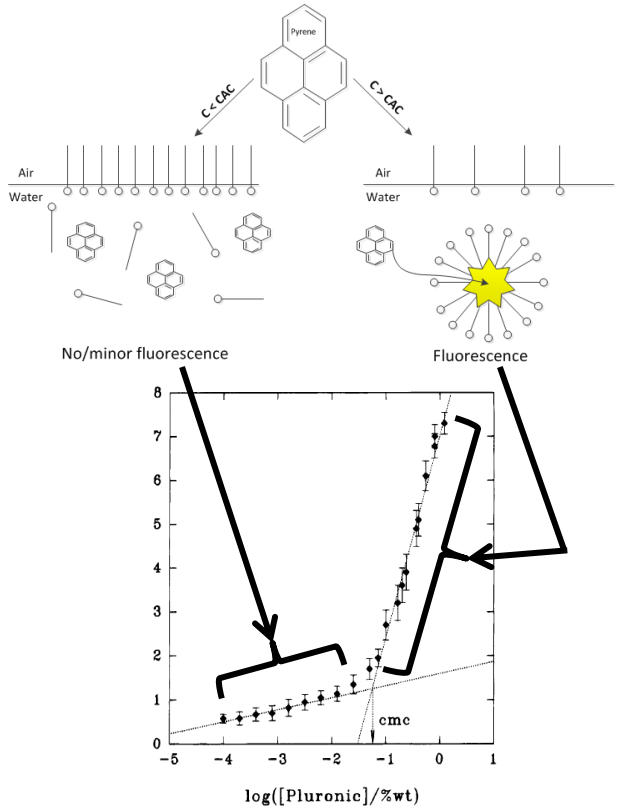

Figure 2.3: *Simple schematic depicting the fluorescence quenching method, in which pyrene is used to determine the critical aggregation concentration (CAC) of a surfactant. The plot below the figure shows relative fluorescence intensity versus the log of the surfactant concentration (Kabanov, 1995). The intersection of the two linear regions is the CAC (here referred to as the critical micelle concentration, CMC).*

Sample preparation was done by making stock solutions containing 10^{-4} mg/mL solutions of pyrene in water and using them to make serial dilutions of surfactants. Surfactants tested included Triton X-100 (Fisher Scientific, Hampton, NH), the cleavable triblocks (CTs) synthesized by Dr. Karl Schilke, and the PEO-PBD-PEO triblocks (Hillmeyer Lab Group, Univ. of Minnesota).

Dilutions were done in 2-mL microcentrifuge tubes (three sets for each surfactant to assess sample variation). The tubes were covered to minimize light exposure and incubated at 35 °C for about 24 hr to allow for equilibrium to be obtained. Samples were then removed from the incubator and moved to a separate lab to allow for fluorescence analysis with a Horiba FluoroLog 3 flourospectrometer with a MicroMax microwell-plate reader (Horiba Scientific, Edison, NJ). The utilized excitation and emission wavelengths were 338 nm and 395 nm, respectively. It should be noted that emission spectra were taken for each test; the largest emission peak that stayed at a fairly constant wavelength across the dilution schemes was at 395 nm. Plating of the dilutions into a 96-well plate was then done, in which two 200-μL samples were taken from each tube to assess instrument error. Reading of the 96-well plate produced fluorescence intensity data which was used to determine the CAC of each surfactant.

2.3 *Hydrophobic region of brush layer*

It is know that Pluronic coatings confer hydrophilic qualities to hydrophobic surfaces. However, there have been multiple findings that point toward the existence of a hydrophobic layer in these coatings. Evidence to this fact has been found in multiple experiments; for example, experiments have been done in which antibiotics

molecules have been “loaded” into Pluronic-coated surface layers (Lampi 2012). This evidence of a hydrophobic region in the surface coatings has not been shown directly.

It was proposed that the molecule pyrene, the same molecule used in the CAC determination tests, be used to prove the existence of this hydrophobic layer. Pyrene is known to fluoresce in hydrophobic environments, so a solution of pyrene should show more intense fluorescence when in contact with a Pluronic-coated surface than when in contact with a bare surface.

Before this test, however, it was proposed that this theory would be stronger with a parallel test run to give evidence of brush layer formation at the same concentrations. Thus, an experiment utilizing β-galactosidase adsorption to silica surfaces was designed.

For the β-galactosidase tests, silica wafers were first prepared for coating. Wafers were cut into strips of approximately 1.4 by 6 cm with a tungsten-tipped etching tool. The strips were then cleaned with an RCA wash, followed by silanization with trichlorovinylsilane (TCVS). Two strips each were then placed in solutions of Pluronics® F-68, F-108, and F-127 just below their CACs and incubated overnight on a shake-plate at 50 rpm to coat the strips. The strips were then rinsed using 20 mM phosphate citrate buffer (PCB) at pH 4.5. Two strips were incubated at the same time in just PCB to serve as uncoated references. The strips were then irradiated with 0.3 MRad γ-radiation to covalently bond the triblocks to the strips. Half of the strips were placed in petri dishes filled with 1 mg/mL β-galacosidase in PCB, while the other half were placed in petri dishes filled with PCB as controls. The strips were incubated in these solutions overnight on a shake plate at 50 rpm, and then

they were rinsed with PCB. Clean, sterile o-rings were placed on a clean, sterile polycarbonate surface in such a way that three o-rings would be covered by a single silica strip. These o-rings were each filled with 300 μL of 1 mM oNPG in PCB and the rinsed strips were each placed on three o-rings and tapped lightly to seal them. After incubation at 37 °C for about three hours, the strips were carefully removed. To each well of a 96-well plate, 160 μL of 100 mM, pH 9.5 sodium borate buffer was added to raise the pH of each sample. Then 80 μL of sample from each o-ring was pipetted into a separate well of the 96-well plate. This would cause color change in the o-rings in which b-galactosidase hydrolyzed the oNPG to oNP and galactose. Thus, examination of absorbance of light at 405 nm would show the extent of β-galactosidase activity, which would give an idea of the protein repulsive character of the coating. This procedure was repeated for coatings made with solutions at concentrations 100 times diluted from the CAC.

Next, the hydrophobic layer theory was tested by creating solutions of Pluronic-coated and uncoated nanoparticles. A solution of 10 mg/mL Aerosil R816 silica nanoparticles were made in 10 mM, pH 7.4 PBS. Pluronics® F-68, F-108, and F-127 were added to 4 mL of the nanoparticle solution in separate containers to give Pluronic concentrations near the CAC of the Pluronic. Separate solutions of nanoparticles were coated with F-68 at 100 mg/mL, F-108 at 45 mg/mL, and F-127 at 7 mg/mL. These solutions were left in 6-mL test tubes on an agitation plate overnight. After incubation, solutions were pipetted into 4, 2-mL microcentrifuge tubes with 1 mL solution each. These tubes were centrifuged at 10,000 rpm for 20 min, and then the supernatant was pipetted out and the solutions were resuspended in 1 mL fresh

PBS. This centrifugation and resuspension procedure was repeated 2-3 times to remove any Pluronic not adsorbed to the nanoparticles. After the final resuspension, the solutions were stored at 10 °C.

A 1 mg/mL solution of pyrene was made in 10 mL dimethyl sulfoxide (DMSO). Dilutions of this solution were made using the uncoated and coated nanoparticle solutions to create solutions of 10 mg/mL nanoparticles with 10^{-4} mg/mL pyrene. Six 200-μL samples from each solution were transferred to a 96-well plate along with a nanoparticle solution without pyrene to account for any fluorescence of the nanoparticles. The well plate was then covered and incubated at 35 °C for 24 hr and then analyzed with a fluorometer. The well plate was analyzed using the same settings as with the CAC determination tests. The procedure was then repeated for coatings made with solutions at concentrations 100 times and 10,000 times diluted from the CAC.

3 RESULTS AND DISCUSSION

3.1 *Membrane permeability*

The data for all of the urea permeability tests were organized into four separate plots: one comparing the two polyacrylonitrile membranes (AN69 and AN69-ST), one for tests done with and without irradiation or triblock coating, one for tests done with and without added BSA, and one for tests done with and without added fibrinogen. The data is summarized in Figures 3.1 and 3.2. In the legends, UC refers to the urea chamber and Res refers to the reservoir.

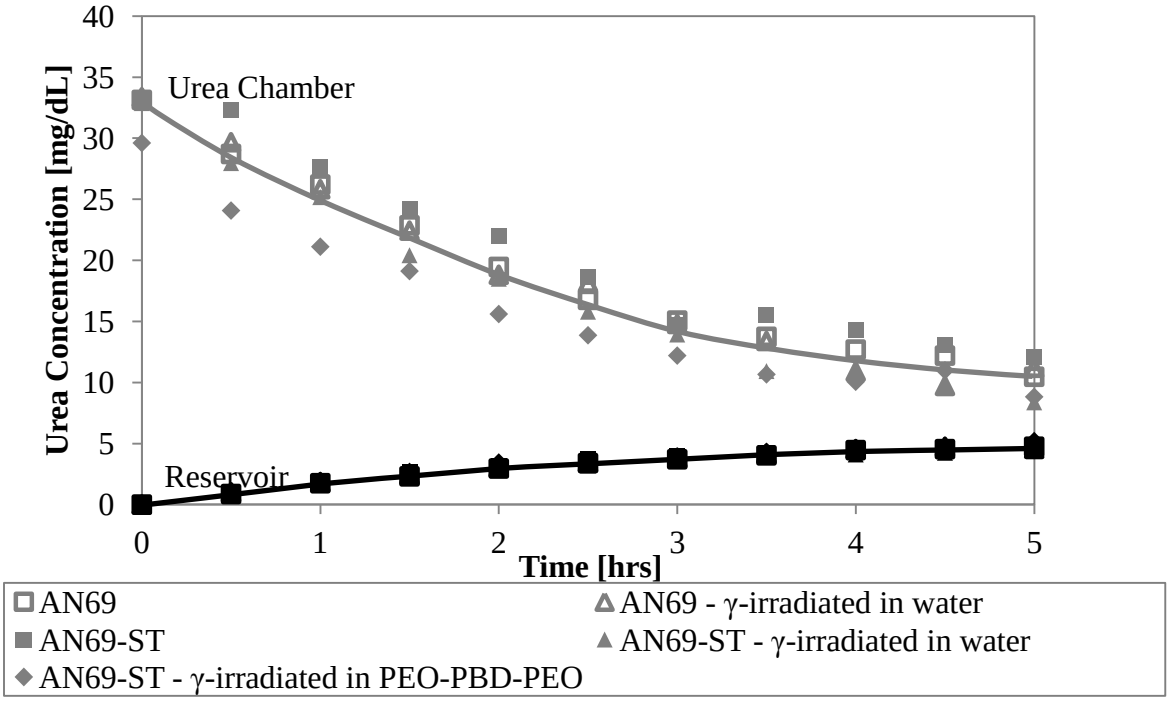

Figure 3.1: *Comparison of urea transport through AN69 and AN69-ST membranes (untreated, γ-irradiated in water, and triblock-coated).*

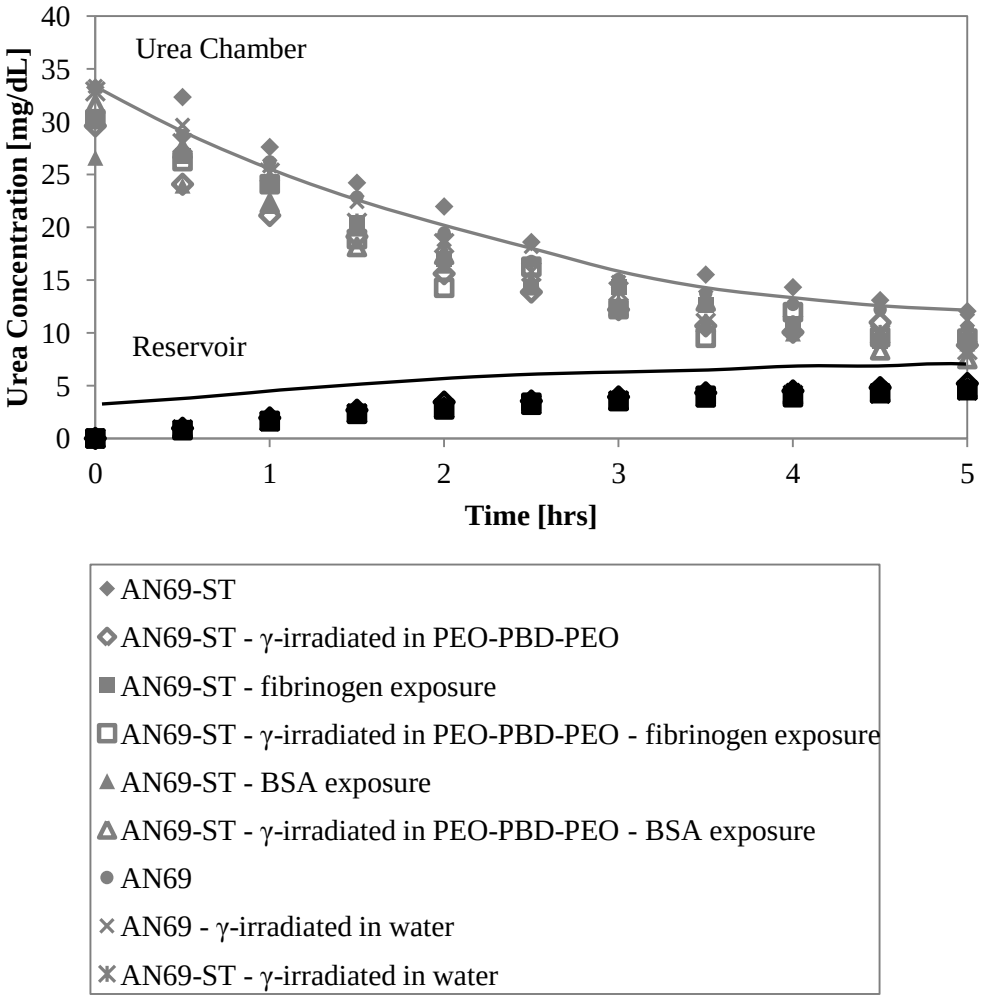

Figure 3.2: *Comparison of urea transport through untreated and triblock-coated membranes, both with and without addition of selected proteins to solutions.*

Although all tests were done with a starting urea concentration of 30 mg/dL, the sensitivity of the assay to time ended up giving values slightly above or below this value. This is not a problem, however, as the trend of the data is more important than the actual values. Thus, data is given relative to show the trend in data.

It can be seen from the figures that there is minimal change in relative amounts of urea allowed to permeate the membrane between each case. Figure 3.1 suggests that the addition of the PEI layer on the AN69-ST does not affect urea

transport. Figure 3.2 suggests that the PEO-PBD-PEO coating and the γ-irradiation don't hinder urea transport through the AN69-ST membrane. Figures 3.3 and 3.4 suggest that neither the presence of BSA nor the presence of fibrinogen in solution affect the urea transport through the AN69-ST membranes. All of these results are encouraging, suggesting that the use of AN69-ST membranes in hemodialysis devices to be coated with triblocks for biocompatibility poses no great hindrance to uremic solute transport.

3.2 *CAC*

The data from the fluorescence tests of the CAC values for the cleavable triblocks are summarized in Figure 3.5. The CAC values determined by these plots are displayed in Table 3.1.

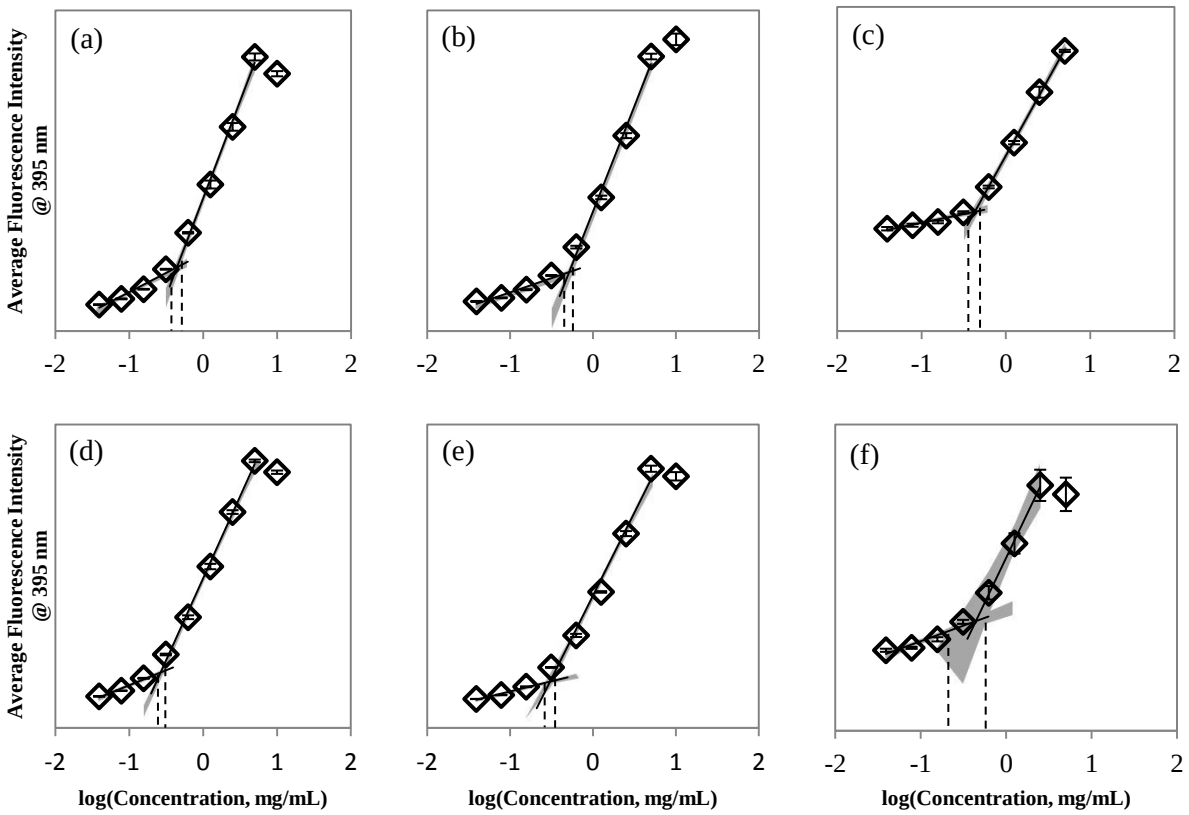

Figure 3.3: *Plots of average fluorescence intensity vs. log of surfactant concentration for cleavable triblocks. Different graphs correspond to triblocks with different conformations: (a) 121, (b) 222, (c) 525, (c) 131, (d) 232, and (e) 535. Black lines show the linear regions of the plots, while grey shaded regions and dotted lines show the 95% confidence regions for determination of values for critical aggregation concentration (CAC). Error bars denote standard error for each point.*

Table 3.1: *Mean values for critical aggregation concentration (CAC) of cleavable triblocks. Values and errors were determined using the 95% confidence bands of the fluorescence intensity plots in Figure 3.5.*

Triblock Designation	CAC Range, mg/mL
CT121	0.15 ± 0.06
CT131	0.42 ± 0.22
CT222	0.35 ± 0.18
CT232	0.33 ± 0.17
CT525	0.43 ± 0.07
CT535	0.43 ± 0.23

There is no large trend in the CAC values of the CTs, but the triblocks with 2kDa centerblocks tend to have lower CAC values than those with the 3 kDa centerblocks. This is expected, due to the fact that the hydrophobic centerblock is known to be the primary force in the aggregation of PEO-based triblocks (Hamley 2005).

Figure 3.6 shows the results for the fluorescence determination of the CAC for the Hillmeyer triblocks. Using the 95% confidence bands, the CAC was calculated to be 2.2 ± 0.3 mg/mL. As this triblock shows great promise for future use, this information will be very useful for coating efficiency.

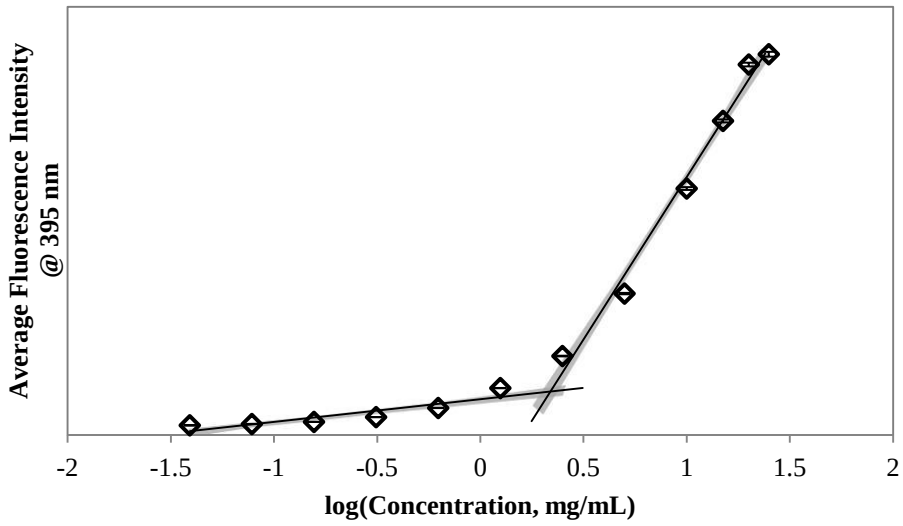

Figure 3.4: *Graph of pyrene fluorescence intensity versus log of Hillmeyer triblock concentration in water. Errors bars show the standard error of each concentration. The gray shaded areas depict the 95% confidence bands, which were used to calculate a CAC of 2.2 ± 0.3 mg/mL.*

Overall, the information given by these tests can be used by future users of the triblocks to help make efficient surface coatings, due to the fact that more effective coatings are made just below the CAC.

3.3 *Hydrophobic region of brush layer*

The results of the β-galactosidase testing can be seen in Figure 3.7. It is clear from the plot that making coatings just below the CAC promotes formation of protein-repellant brush layers. On the other hand, coatings made with 100 times diluted solutions showed no evidence of brush layer formation.

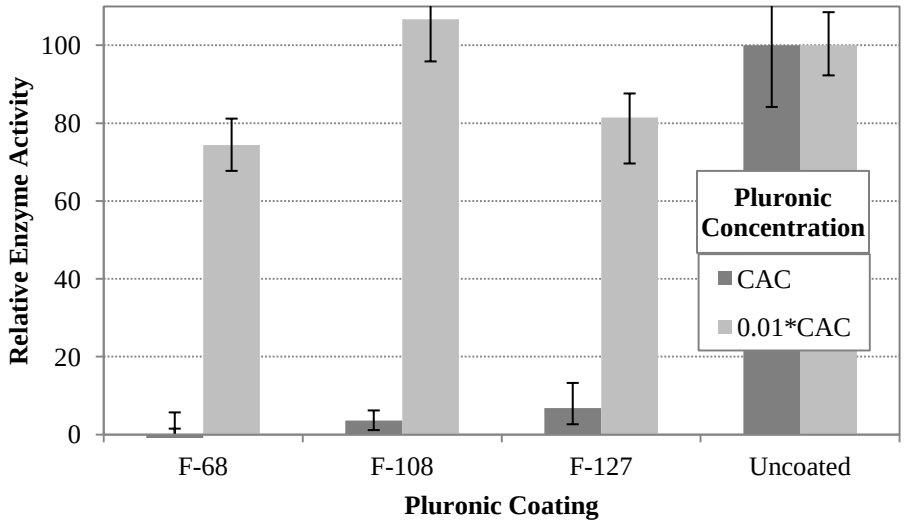

Figure 3.5: *Plot of relative activity of β-galactosidase for different types of Pluronic coatings on silicon. Coatings were made at different concentrations, denoted by the dilution factors. The dilution scheme is based on the CAC value for each Pluronic. The error bars show the minimum and maximum values for each data set of three samples.*

The results of the fluorescence analysis of Pluronic-coated R816 Aerosil nanoparticles can be seen in Figure 3.8. For the F-108 and F-68 coatings, a drastic decrease in fluorescence intensity is seen from coatings made just below the CAC to

coatings made at concentrations 100 and 10,000 times diluted. This observation points toward the presence of a hydrophobic region within the brush created by the coatings just below the CAC. The less drastic decrease in intensity seen for the F-68 coatings is a result of the higher CAC of the F-68.

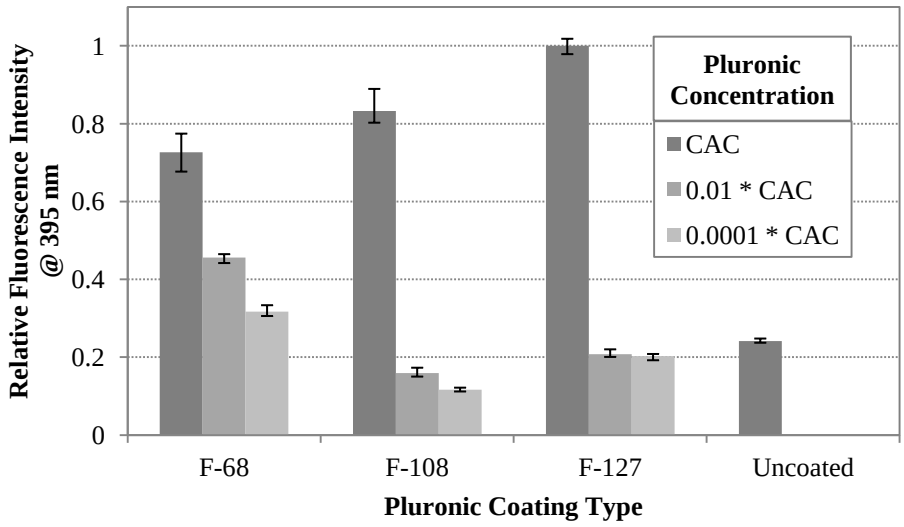

Figure 3.6: *Plot of relative fluorescence intensity of pyrene at 395 nm for different types of Pluronic coatings on R816 nanoparticles. Coatings were made at different concentrations, denoted by the dilution factors. The dilution scheme is based on the CAC value for each Pluronic. The error bars show the minimum and maximum values for each data set of three samples.*

4 CONCLUSION

Many characteristics of triblock surfactants were explored in this research, including their effects on transport through hemodialysis membranes, their aggregation behavior, and their formation of brush layers with hydrophobic layers. It was shown that AN69-ST membranes coated with PEO-PBD-PEO triblock copolymers did not show significant differences in urea transport. The CACs for cleavable triblocks and the novel

PEO-PBD-PEO triblocks were also determined using pyrene fluorescence. In addition, the presence of a hydrophobic layer in the brush layers created by Pluronics® F-68, F-108, and F-127 was proven using pyrene fluorescence of coated R816 Aerosil nanoparticles. All of this information provides a comprehensive look at characteristics of triblock surfactants for use in future research interests.

5 REFERENCES

Hamley, I.W. (2005). *Block copolymers in solution: Fundamentals and applications*. Hoboken: Wiley.

Jung, D., Biggs, H., Erikson, J., Ledyard, P. U. (1975). New colorimetric reaction for end-point, continuous flow, and kinetic measurement of urea. *Clinical Chemistry* (Vol. 21, pp. 1136-1140).

Kabanov, A.V., Nazarova, I.R., Astafieva, I.V., Batrakova, E.V., Alakhov, V.Yu., Yaroslavov, A.A., Kabanov, V.A. (1995). Micelle formation and solubilization of fluorescent probes in poly(oxyethylene-b-oxypropylene-b-oxyethylene) solutions. *Macromolecules* (Vol. 28, pp. 2303-2314).

Lampi, M. (2012). *Molecular origins of peptide entrapment within polyethylene oxide brush layers* (OSU Honors Thesis). Retrieved from OSU Library Scholar's Archive.

Lee, J., Martin, P. A., Tan, J. S. (1989). Protein adsorption on pluronic copolymer-coated polystyrene particles. *Journal of Colloid & Interface Science* (Vol. 131, pp. 252-266).

McPherson, T.B., Shim, H.S., and Park, K. (1997). Grafting of PEO to glass, nitinol, and pyrolytic carbon surfaces by gamma irradiation. *J. of Biomedical Materials Research* (Vol. 38, pp. 289-302).

Zawada, R. J. X., Kwan, P., Olszewski, K. L., Llinas, M., Huang, S. (2009). Quantitative determination of urea concentrations in cell culture medium. *Biochemistry & Cell Biology* (Vol. 87, pp.541-544).

6 APPENDIX A

Short communication

SURFACE and INTERFACE ANALYSIS

Received: 19 February 2012 Revised: 17 July 2012 Accepted: 21 August 2012 Published online in Wiley Online Library

(wileyonlinelibrary.com) DOI 10.1002/sia.5168

Direct imaging of the surface distribution of immobilized cleavable polyethylene oxide-polybutadiene-polyethylene oxide triblock surfactants by atomic force microscopy

Karl F. Schilke,* Joshua L. Snider, Lauren E. Jansen and Joseph McGuire

Cleavable amphiphilic triblock surfactants with methoxypolyethylene oxide (PEO) side-chains attached to polybutadiene (PBD) center blocks by ester linkages were synthesized. The PEO–PBD–PEO triblocks were adsorbed on hydrophobic silicon wafers and covalently stabilized by γ-irradiation. The PEO side-chains were then cleaved from the PBD backbones by acid hydrolysis. Decoration of the immobilized centerblocks with β-cyclodextrin allowed direct imaging by standard atomic force microscopy techniques. Widely varied surface coverage, layer morphology and distributions of the PBD centerblocks were observed on surfaces coated with different triblock concentrations and PEO:PBD ratios. Surfaces coated from 1 mg/mL solutions of triblocks (near the critical aggregation concentration (CAC), 0.28–0.53 mg/mL) were sparsely coated, and triblocks containing 75–85% PEO exhibited negligible surface coverage, possibly due to poor adsorption or facile desorption during rinsing. Dense surface packings, albeit some with evident defects sufficiently large to allow for protein adsorption, were produced from 10 mg/mL triblock solutions (an order of magnitude above the CAC). This proof-of-concept report describes a method that may be useful in optimizing surface coatings on model substrates, and thus lend insight into optimization of coating conditions for economical production of non-fouling triblock-based PEO coatings on clinically relevant biomedical materials. **Copyright © 2012 John Wiley & Sons, Ltd.**

Supporting information may be found in the online version of this article.

Keywords: cleavable surfactants; PEO–polybutadiene–PEO triblocks; atomic force microscopy; non-fouling coatings; β-cyclodextrins; pyrene fluorescence

Introduction

Surfaces of biomaterials must resist adsorption of blood proteins or adhesion of bacterial cells. Economical production of non-fouling layers on biomedical polymers and other materials used in clinical practice will likely require new materials, coating protocols and optimization strategies. Imaging of the surface density and distribution of candidate surface coatings is important for optimization of coating conditions, but typically presents substantial experimental difficulties. In this work, we describe a method that directly addresses the challenges of visualizing the surface morphology and density of such non-fouling pendant polymer coatings. This approach may be useful in development and optimization of a variety of surface coating methods.

Coatings of pendant hydrophilic polymers, including polyethylene oxide (PEO), can prevent adsorption of cells and proteins by steric hindrance and other mechanisms. Chain length and packing density strongly affect the protein-repellent capability of PEO layers.[1–8] Despite the well-known non-fouling characteristics of PEO brushes, the protective effect is rarely absolute – a small amount of protein is typically observed at the surface.[9,10] The amount of adsorbed protein depends on the density and uniformity of the pendant polymers, and hence depends strongly on the surface coating conditions.

Pendant PEO layers may be produced by a variety of 'graft-to' reactions of end-modified PEO,[1,3,11–13] or adsorption of 'bottle-brush' graft copolymers (e.g. polylysine–*g*–PEO) on negatively charged surfaces.[14,15] Dense PEO layers can also be formed by simple adsorption of the polypropylene oxide (PPO) centerblock of amphiphilic PEO–PPO–PEO triblock copolymers onto a hydrophobic surface from an aqueous solution.[16–18] However, adsorbed triblocks may be competitively displaced by exposure to blood proteins. Stable, covalently linked PEO coatings are easily formed by irradiation of PEO–PPO–PEO triblocks on vinyl-functionalized model surfaces under water.[3,19–21] Radiolysis of water produces radicals that transfer to the –C=C– double bonds in the surface vinyl groups,[22,23] which attack the neighboring adsorbed PPO chains to form covalent bonds that anchor the triblocks to the surface. Reaction of these polymer-bound radicals with water and dissolved O_2 may also produce hydroxyl (—OH), carboxylic (—COOH) groups and other oxidized species.[5,12,22,24]

Many materials used in biomedical applications (e.g. polyurethanes) are not amenable to activation of the surface itself. Triblocks made of PEO and polybutadiene (PBD) have many double bonds in the hydrophobic PBD centerblock. This allows

* *Correspondence to: Karl F. Schilke, Gleeson Hall Rm. 102, Oregon State University, Corvallis, OR 97331, USA. E-mail: karl.schilke@oregonstate.edu*

School of Chemical, Biological and Environmental Engineering, Oregon State University, Corvallis, OR 97331, USA

 Copyright © 2012 John Wiley & Sons, Ltd.

covalent immobilization of PEO–PBD–PEO triblocks on practically any unmodified hydrophobic surface by γ-irradiation in water.[3,5,10,12] Toxic and expensive cross-linkers are not required, and immobilization of the triblocks could occur during conventional sterilization by γ-irradiation. These points make triblock-based coatings very attractive for use on commercial biomedical devices.

Pendant PEO layers formed by irradiation-stabilized triblocks effectively prevent the adsorption of large proteins from solution. However, experimental and theoretical evidence suggests that these layers are less effective at repelling small peptides. Theoretical models predict that proteins smaller than the average chain spacing can intercalate into brush layers.[8,25,26] Moreover, the immobilized triblock-based brushes are not expected to be perfectly distributed and will likely have bare spots. These defects are responsible for the observed adsorption of proteins to PEO-coated surfaces.[27] For instance, the small lantibiotic peptide nisin (3.4 kDa) was observed to integrate in multilayer quantities on model surfaces coated with PEO–PPO–PEO triblocks, while bovine serum albumin did not adsorb.[18] Nisin was also observed at PEO–PBD–PEO layers on medical-grade polyurethanes and was apparently protected by the brush from competitive displacement by fibrinogen.[10] The ability of small natural or synthetic biofunctional peptides to integrate into otherwise biocompatible surface coatings suggests a variety of novel strategies for controlled drug release, a subject that is currently under investigation in our laboratory.

Atomic force microscopy (AFM) is commonly used for visualization of surface topography. The PEO coating is most usefully examined in a fully hydrated state, to avoid artifacts caused by the collapse of the extended chains onto the surface during drying. However, the 'fluid surface' of the polymers, variable penetration depth of the tip and entanglement and adhesion between the tip and the polymer chains make this problematic.[28–30] Imaging of pendant polymers under water or solvents is possible, but is generally more difficult than dry samples.[30,31]

Block copolymers with cleavable disulfide linkages (e.g. polystyrene-SS-PEO) have been developed for nanotemplating applications.[32,33] A similar technique was used to eliminate the mobile PEO chains of immobilized triblocks prior to AFM imaging (Fig. 1). Novel triblocks with cleavable ester linkages between the PEO and PBD blocks were synthesized and adsorbed on model hydrophobic surfaces. After immobilization, the ester bonds were hydrolyzed to release the PEO side-chains, leaving the immobilized PBD centerblock polymers on the surface.

Various nanoparticles have been attached to surface-bound polymers to increase their cross-section and spatial contrast under AFM.[34–36] In the present study, the immobilized PBD polymers were decorated with β-cyclodextrins (hydroxyl-rich, 1.7 nm conical molecules, Fig. 1).[37–39] Visualization of the spatial distribution of individual triblock polymers on surfaces can help improve our understanding of the formation and morphology of triblock brush layers, and thus guide efforts to produce more uniform non-fouling coatings on clinically relevant biomedical materials (e.g. polyurethane).

Materials and methods

Complete experimental details are available in the Supplementary Information document.

Preparation of C_{18} substrates

Chips (~1 cm^2) cut from the center of a single oxidized silicon wafer were modified with 5% octadecyltrimethoxysilane (ODTMS, C_{18}) in dry EtOH (25 °C, 3 h) and cured at 150 °C.

Synthesis of cleavable PEO–PBD–PEO triblocks

Cleavable PEO–ester–PBD–ester–PEO triblocks with various PEO:PBD ratios were synthesized in good yield (Fig. 2). Methoxy-PEO (nominal M_n 750, 2000 and 5000 Da) was first carboxylated with excess succinic anhydride[40] and then linked to hydroxyl-terminated (HTPBD) by Steglich esterification with dicyclohexylcarbodiimide and 4-dimethylaminopyridine.[41] The resulting triblocks were purified by precipitation in diethyl ether or hexane, and coded '*CTnmn*', where '*n*' is the approximate M_n of the PEO (~1, 2 or 5 kDa), and '*m*' the PBD M_n (2 or 3 kDa).

Immobilization and cleavage of PEO–PBD–PEO triblocks

All aqueous solutions and rinses were made with HPLC-grade water. C_{18} wafers were incubated with cleavable triblocks (1 or 10 mg/mL) in 5% isopropyl alcohol (IPA) overnight at 25 °C, then gently rinsed with copious water to remove excess triblock. Irradiation in the presence of triblocks has been shown

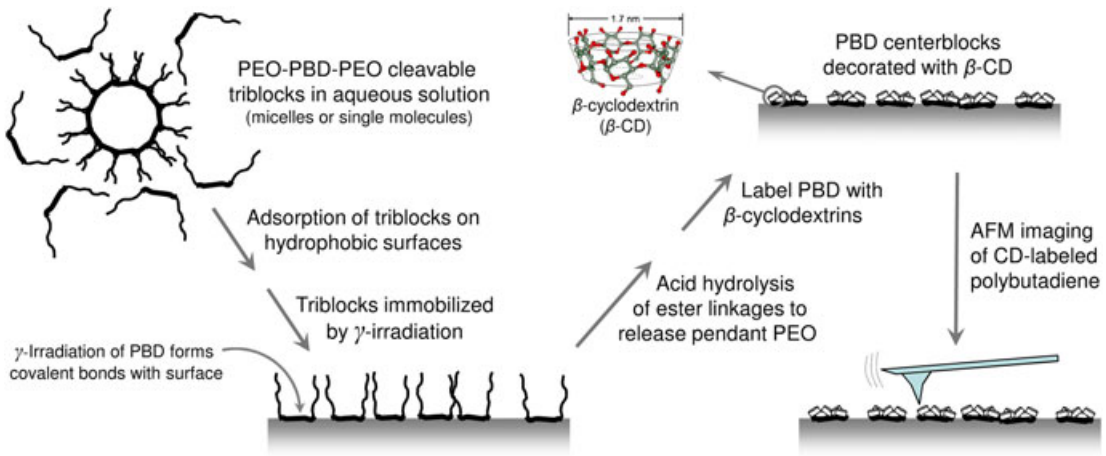

Figure 1. Method for imaging the surface distribution of cleavable PEO–PBD–PEO triblocks on model surfaces.

Copyright © 2012 John Wiley & Sons, Ltd.

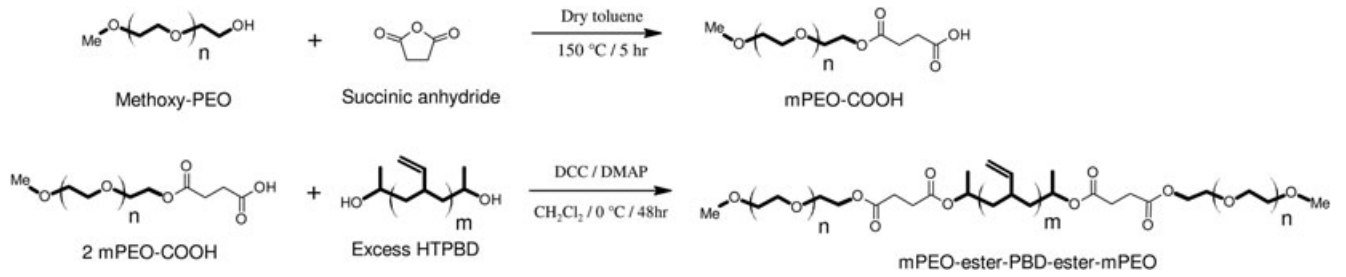

Figure 2. Synthesis of PEO-ester-PBD-ester-PEO triblock surfactants with cleavable ester linkages. Polymer repeat units are emphasized. Polybutadiene is shown with all 1,2 (vinyl) groups for clarity.

to increase protein repulsion,[5] probably by formation of multilayer, cross-linked coatings. Thus, for clarity, we rinsed away all but the surface-adsorbed triblocks. The proposed method should be easily extensible to surfaces irradiated under triblock solutions. Triblock-free controls were also prepared. The wafers were γ-irradiated under water to a total dose of 3 kGy (8 h) to covalently link the adsorbed PBD centerblocks to the C_{18} surface.[3,5,12,42] Ellipsometric measurement of immobilized triblocks showed that they were resistant to elution by sodium dodecyl sulfate (data not shown). After irradiation, control and triblock-coated wafers were treated with 3 M H_2SO_4 (80 °C, 30 min) to cleave the PBD–PEO ester linkages[43] and form –OH groups by addition of water across remaining double bonds. Some of the interblock ester linkages and double bonds may also be hydrolyzed during irradiation.[44,45]

Decoration of immobilized PBD with β-cyclodextrin

The immobilized PBD centerblocks were decorated with β-cyclodextrins (β-CD, Fig. 3). Irradiated chips were incubated with 0.1 M 2,4-tolylene diisocyanate in toluene (3 h), rinsed thoroughly with toluene, and then covered with 50 mg/mL dried β-CD in DMSO for 18 h. Excess β-CD was removed by rinsing sequentially with DMSO and water. The decoration reactions were performed in anhydrous solvents under dry N_2.

Measurement of critical aggregation concentration

The critical aggregation concentrations (CAC) of cleavable triblocks in 5% IPA solutions of various concentrations were determined at 25 °C using the pyrene fluorescence method.[46,47] In solutions above the CAC, pyrene is taken up into the hydrophobic core of the micelles, and its fluorescence greatly increases due to the change in the polarity of the microenvironment.

AFM imaging of β-CD-decorated polymers

Chips were rinsed thoroughly with HPLC water, and blown dry with filtered N_2 immediately before imaging in intermittent contact ('tapping') mode with an Asylum Research MFP3D microscope (Santa Barbara, CA) and TAP300Al-G probes (BudgetSensors, Sophia, Bulgaria). Images (1 × 1 μm) of the surface topography were generated at several locations chosen at random near the center of the chips. Representative images were flattened by plane-fitting and rendered with ARgyle Light (Asylum Research) at 1:1 *z*-aspect, with specularity added to enhance the surface texture.

Calculation of surface roughness and coverage

Surface roughness was calculated from AFM images using the MFP3D software, with pixels corresponding to presumed contaminants ($z > 8$ nm) masked out. Isometric grayscale 'top-down' images of the surfaces were also exported to ImageJ,[48] and converted to binary by automatic thresholding. Manual thresholding was necessary at high surface coverage. The calculated areal densities are reported without correction for tip radius effects.

Results and discussion

CAC of PEO-PBD-PEO triblocks

The CAC of the synthesized PEO-PBD-PEO triblocks under coating conditions were below 1 mg/mL (Table 1). The triblocks with 3 kDa PBD centerblocks exhibited a slightly lower CAC (higher propensity to aggregate) than those with smaller (2 kDa) PBD blocks. The hydrophobe block primarily drives aggregation of PEO-based triblocks, and its size thus largely determines the CAC of the polymer.[49]

Immobilization of PEO–PBD–PEO triblocks

C_{18} wafers were coated overnight at 25 °C from PEO–PBD–PEO triblock solutions in 5% IPA. Loosely bound triblocks were removed by sequentially transferring each wafer into pure water (4×), with gentle agitation under the surface. The wafers were then γ-irradiated (^{60}Co, 3 kGy) under water to covalently attach the PBD centerblocks to the C_{18}-modified surface. Bulk water greatly increases the rate of formation of cross-links between the adsorbed PBD and neighboring surface, due to transfer of energy from water-derived radicals to activate the double bond. The PEO side-chains were removed from the immobilized triblocks by acid hydrolysis of the ester bonds. This treatment also catalyzes addition of water across the remaining double bonds, forming additional –OH groups. These polymer-bound hydroxyls were decorated with β-cyclodextrins,[38] 'amplifying'

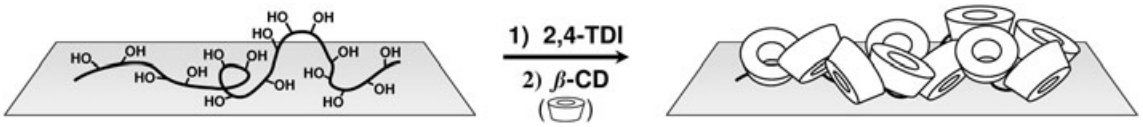

Figure 3. Decoration of immobilized hydroxylated PBD backbone with β-cyclodextrins prior to AFM imaging.

Copyright © 2012 John Wiley & Sons, Ltd.

Table 1. CAC of cleavable PEO-PBD-PEO triblocks in 5% isopropyl alcohol, as measured by pyrene fluorescence ($n = 6$)

Triblock	CAC (mg/mL)	Triblock	CAC (mg/mL)	Triblock	CAC (mg/mL)
CT121	0.45 ± 0.07	CT222	0.52 ± 0.07	CT525	0.43 ± 0.07
CT131	0.28 ± 0.03	CT232	0.31 ± 0.05	CT535	0.41 ± 0.20

the polymer to a height of 2–4 nm (Fig. 3), and then imaged with AFM.

AFM imaging of immobilized triblock backbones

Control surfaces

Pristine C_{18} wafers were very flat, with an RMS roughness of ~0.4 nm. The γ-irradiation and hot acid treatments only slightly increased the surface roughness of the C_{18} coatings. Unlike the islands typically observed with small silanes such as aminopropyltrimethoxysilane,[50,51] the long alkyl tails of the C_{18} silanes tend to self-assemble into smooth, hydrophobic and semi-crystalline monolayers, which exclude ions (e.g. HO^-) that could cause etching.[52,53] Little or no β-CD was observed on triblock-free control wafers.

Surfaces coated with 1 mg/mL triblocks

Surface coverage was sparse for coatings from triblocks incubated at 1 mg/mL (Fig. 4). Most islands are 3–5 nm in height, which is consistent with immobilized β-cyclodextrins (i.e. 1.7 nm diameter with a ~0.8 nm linker; see Fig. 3), but peaks up to 8 nm high probably represent contaminants. Triblocks with 3 kDa PBD backbones produced similar or slightly higher surface coverage than 2 kDa PBD, but without a substantial improvement in uniformity. These sparse layers are consistent with a report that surfaces coated with PEO_{2000}–PBD_{750}–PEO_{2000} triblocks from aqueous solutions at concentrations below 5 mg/mL provided little protection against platelet adhesion.[5]

Surprisingly, there was little evidence of immobilized triblocks on the surfaces coated with either CT525 or CT535 (the few observed tall features are 8–12 nm high, and probably represent contaminants). The PEO blocks of these surfactants make up 75–85% of the polymer, suggesting that adsorption might be hindered by the less-polar 5% IPA solution, or desorption of the triblocks from the surface during rinsing with water. Foams of these triblocks were somewhat less stable than smaller triblocks (data not shown), indicating reduced amphiphilic character. However, we recently reported[10] the repulsion of fibrinogen by γ-immobilized PEO–PBD–PEO triblocks with an even higher PEO:PBD ratio (~90% PEO).

Surfaces coated with 10 mg/mL triblocks

AFM images (1×1 μm) of surfaces coated from 10 mg/mL triblock solutions (Fig. 5) were strikingly different from the 1 mg/mL coatings. The 10 mg/mL triblock solutions were slightly opalescent, suggesting the presence of large micelle structures in the solutions. The smallest triblocks (CT121 and CT131) produced relatively large-scale surface patterns consistent with aggregates or islands of adsorbed surfactants. The sweep radius of PEO[54] is approximately $R_g \approx 0.181N^{0.58}$ (nm), so the 750 Da ($N \sim 17$) PEO of intact CT121/131 is expected to sweep only ~1 nm. Thus, volume exclusion by the PEO side-chains cannot be responsible for bare spots that ranged in size from several nm to ~50 nm (accounting for tip radius

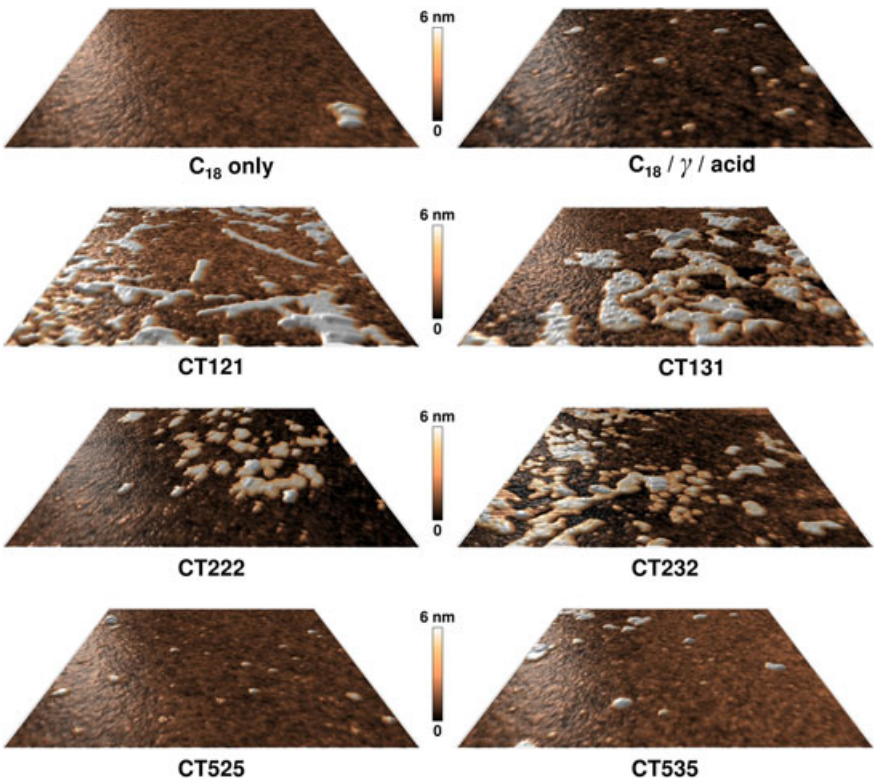

Figure 4. AFM images (1×1 μm) of controls and β-CD-labeled immobilized polybutadiene backbones of PEO–PBD–PEO triblocks deposited from 1 mg/mL aqueous solution.

Copyright © 2012 John Wiley & Sons, Ltd.

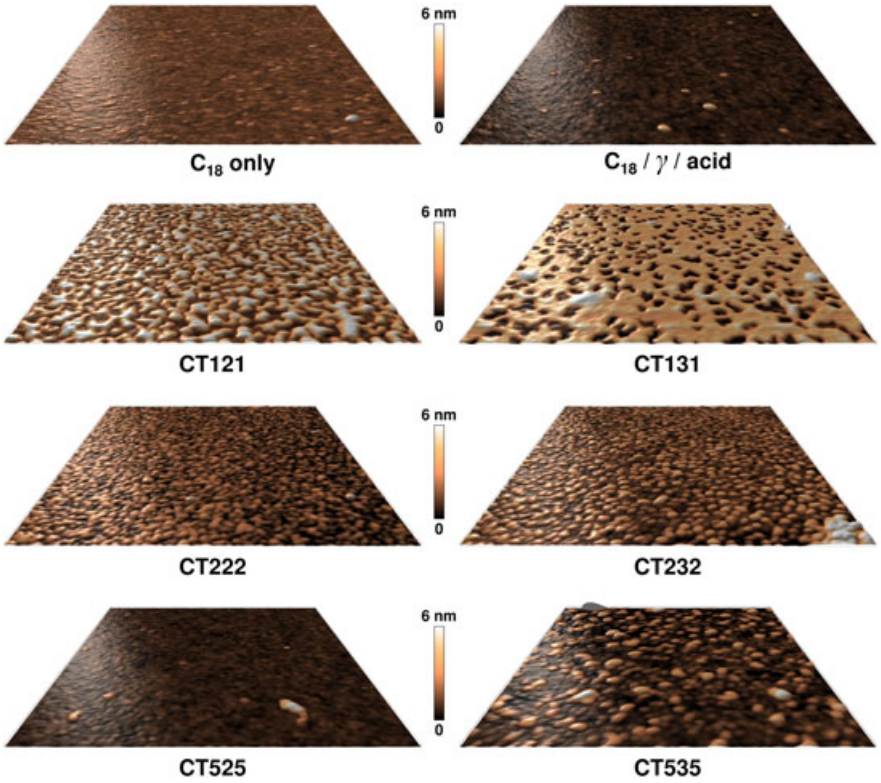

Figure 5. AFM images (1 × 1 μm) of controls and β-CD-labeled immobilized polybutadiene backbones of PEO–PBD–PEO triblocks deposited from 10 mg/mL aqueous solution.

effects). The patterns may be due to the adsorption of triblocks from lamellar, worm-like, or circular micellar conformations caused by the relatively large hydrophobic PBD centerblock and short PEO chains.[49,55] Phase separation may also occur during self-assembly; indeed, the surface features are morphologically similar to those observed in spin-cast thin films of diblock copolymers.[33,56] The underlying hydrophobic surface is partially exposed and thus may support low levels of protein adsorption.[9,10] The measured heights of these coatings also range from 2 to 5 nm, consistent with β-cyclodextrins immobilized on polymers.[38]

In contrast, however, the CT222 and CT232 surfaces exhibited a highly uniform, tight surface distribution with few defects. Such coatings would be expected to provide good biocompatibility. Aggregate sizes increased with larger PBD backbones, suggesting a more favorable association between the more hydrophobic triblocks. Presumably, the longer (2 kDa) PEO chains inhibit the aggregation observed with smaller triblocks during the self-assembly process, producing a more regular and compact surface structure. Associations of the PEO chain ends are favored by the terminal CH_3O– groups,[7] and can provide hydrophobic regions on the brush that may promote adsorption of proteins.[6] These interactions may be involved in formation of the different spacings of the features of coatings with the same PBD centerblock.

As with the 1 mg/mL solution, no triblocks were observed on 10 mg/mL CT525-coated surfaces, again possibly because of the high PEO:PBD ratio. In contrast, CT535 produced uniform, dense layers at this concentration, with morphology similar to that of 10 mg/mL CT232. This suggests that the surface spacing is a strong function of PEO chain length (or its volume exclusion), up to some critical chain length. Indeed, this is consistent with observations that protein repulsion of PEO brushes is independent of PEO chain length above about 2–3 kDa.[6,7,57]

Surface coverage and roughness

Calculated surface coverages and RMS roughness for each treatment are provided in Table 2. Coverage values are approximate due to tip radius effects and the subjective nature of the binary thresholding procedure applied to grayscale images, particularly at high triblock densities.

The low surface coverage observed on surfaces coated with 1 mg/mL triblocks may be partially due to concentration effects. All of the triblocks exhibit CAC's near 1 mg/mL (Table 1), so at 1 mg/mL, they may be absorbed on the surface as single chains or 'pre-micelle aggregates' that produce sparse morphologies. In contrast, at concentrations much greater than the CAC

Table 2. Surface coverage (area %) and RMS roughness (nm) of ß-CD-labeled triblocks on representative 1×1 μm areas, calculated from AFM image data. Surface coverages are approximate due to tip radius and grayscale image thresholding effects. Roughness data excludes pixels corresponding to presumed contaminants ($z > 8$ nm)

	1 mg/mL PEO–PBD–PEO		10 mg/mL PEO–PBD–PEO	
Treatment	**Coverage (%)**	**Roughness (nm)**	**Coverage (%)**	**Roughness (nm)**
C18 only	<1%	0.32	< 1%	0.42
C18 / γ / acid	3%	0.82	4%	0.32
CT121	27%	2.22	45%	1.64
CT131	25%	2.28	77%	1.46
CT222	16%	1.65	65%	0.83
CT232	24%	1.95	50%	1.03
CT525	2%	0.86	< 1%	0.35
CT535	5%	1.19	60%	1.50

Copyright © 2012 John Wiley & Sons, Ltd.

(e.g. 10 mg/mL), dense structures of adsorbed unimers and micelles are expected.[31,49] This is consistent with the structures observed in Figs. 4 and 5.

In addition, the C_{18} wafer surfaces that were coated with 1 mg/mL triblocks remained substantially hydrophobic. Despite efforts to maintain a wetted surface on these wafers, the water tended to bead up between the wash cycles. These surfaces were thus repeatedly exposed to a moving air–water interface, which may have partially desorbed the triblocks. In contrast, the wafers incubated with 10 mg/mL triblocks were much more wettable, consistent with a denser PEO layer, and did not exhibit this behavior.

Conclusions

This proof-of-concept study demonstrates direct visualization of the surface distribution of the isolated centerblock of PEO–PBD–PEO triblock layers. Such triblocks can be used to produce stable, protein-repellent layers on a wide variety of hydrophobic surfaces, without use of expensive or toxic reagents. Minimizing the presence of layer defects or 'holes' that may support protein adsorption is of great importance for biomaterials applications. Surface coverage of adsorbed triblocks could be improved by addition of salts (e.g. K_2SO_4) or poor solvents (e.g. ethanol) which collapse the PEO chains,[58] or by changing the adsorption temperature or triblock concentration.[5,54]

This analytical method provides a practical framework for optimizing the distribution of triblock-based PEO layers on model surfaces. Further work will investigate the effects of solution conditions (e.g. temperature, salts, etc.) on the coating morphology and might benefit from the use of finer AFM tips or a smaller labeling molecule (e.g. nitrophenyl isocyanate), which would obscure less of the fine detail of the immobilized polymers. Studies of protein adsorption with respect to triblock layer morphology will provide insight for the optimization of non-fouling, biocompatible coatings on clinically relevant biomedical materials, and may offer direction for design of new drug delivery strategies.

Acknowledgements

We thank Dr. Ethan Minot for the use of his AFM, and Landon Prisbrey, Matthew Leyden, and Josh Kevek for their invaluable assistance. This work was supported in part by the National Science Foundation, Grant No. CBET-0602718, and the National Institute of Biomedical Imaging and Bioengineering (NIBIB; Grant No. R01EB011567). The content is solely the responsibility of the authors and does not necessarily represent the official view of the NIBIB or the National Institutes of Health.

References

[1] J. G. Archambault, J. L. Brash, *Colloids Surf. B Biointerfaces* **2004**, *33*, 111.
[2] A. Halperin, *Langmuir* **1999**, *15*, 2525.
[3] T. B. McPherson, H. S. Shim, K. Park, *J. Biomed. Mater. Res.* **1997**, *38*, 289.
[4] S. T. Milner, *Science* **1991**, *251*, 905.
[5] Y.-C. Tseng, T. McPherson, C. S. Yuan, K. Park, *Biomaterials* **1995**, *16*, 963.
[6] L. D. Unsworth, H. Sheardown, J. L. Brash, *Biomaterials* **2005**, *26*, 5927.
[7] L. D. Unsworth, H. Sheardown, J. L. Brash, *Langmuir* **2008**, *24*, 1924.
[8] F. Fang, J. Satulovsky, I. Szleifer, *Biophys. J.* **2005**, *89*, 1516.
[9] P. Kingshott, S. McArthur, H. Thissen, D. G. Castner, H. J. Griesser, *Biomaterials* **2002**, *23*, 4775.
[10] K. F. Schilke, J. McGuire, *J. Colloid Interface Sci.* **2011**, *358*, 14.
[11] G. L. Kenausis, J. Vörös, D. L. Elbert, N. Huang, R. Hofer, L. Ruiz-Taylor, M. Textor, J. A. Hubbell, N. D. Spencer, *J. Phys. Chem. B* **2000**, *104*, 3298.
[12] A. Kidane, T. McPherson, H. S. Shim, K. Park, *Colloids Surf. B Biointerfaces* **2000**, *18*, 347.
[13] S. J. Sofia, V. Premnath, E. W. Merrill, *Macromolecules* **1998**, *31*, 5059.
[14] R. Michel, S. Pasche, M. Textor, D. G. Castner, *Langmuir* **2005**, *21*, 12327.
[15] M. S. Wagner, S. Pasche, D. G. Castner, M. Textor, *Anal. Chem.* **2004**, *76*, 1483.
[16] J.-T. Li, J. Carlsson, J.-N. Lin, K. D. Caldwell, *Bioconjugate Chem.* **1996**, *7*, 592.
[17] J. A. Neff, K. D. Caldwell, P. A. Tresco, *J. Biomed. Mater. Res.* **1998**, *40*, 511.
[18] Y.-C. Tai, P. Joshi, J. McGuire, J. A. Neff, *J. Colloid Interface Sci.* **2008**, *322*, 112.
[19] K. Park, S. Shim Hong, K. Dewanjee Mrinal, L. Eigler Neal, *J. Biomater. Sci. Polym. Ed.* **2000**, *11*, 1121.
[20] S. Rajam, C.-C. Ho, *J. Membr. Sci.* **2006**, *281*, 211.
[21] M. P. Ryder, K. F. Schilke, J. A. Auxier, J. McGuire, J. A. Neff, *J. Colloid Interface Sci.* **2010**, *350*, 194.
[22] P. Alexander, A. Charlesby, *J. Polym. Sci.* **1957**, *23*, 355.
[23] J. H. O'Donnell, A. K. Whittaker, *J. Polym. Sci., Part A: Polym. Chem.* **1992**, *30*, 185.
[24] A. R. Denaro, G. G. Jayson, *Fundamentals of radiation chemistry*, Butterworth, London, **1972**.
[25] M. Malmsten, K. Emoto, J. M. Van Alstine, *J. Colloid Interface Sci.* **1998**, *202*, 507.
[26] M. Rovira-Bru, F. Giralt, Y. Cohen, *J. Colloid Interface Sci.* **2001**, *235*, 70.
[27] P. Katira, A. Agarwal, H. Hess, *Adv. Mater.* **2009**, *21*, 1599.
[28] G. R. J. Artus, S. Jung, J. Zimmermann, H. P. Gautschi, K. Marquardt, S. Seeger, *Adv. Mater.* **2006**, *18*, 2758.
[29] O. Azzaroni, S. Moya, T. Farhan, A. A. Brown, W. T. S. Huck, *Macromolecules* **2005**, *38*, 10192.
[30] B. Zhao, W. J. Brittain, W. Zhou, S. Z. D. Cheng, *Macromolecules* **2000**, *33*, 8821.
[31] I. W. Hamley, S. D. Connell, S. Collins, *Macromolecules* **2004**, *37*, 5337.
[32] A. Klaikherd, S. Ghosh, S. Thayumanavan, *Macromolecules* **2007**, *40*, 8518.
[33] J.-H. Ryu, S. Park, B. Kim, A. Klaikherd, T. P. Russell, S. Thayumanavan, *J. Am. Chem. Soc.* **2009**, *131*, 9870.
[34] A. Kiriy, G. Gorodyska, N. Kiriy, R. Sheparovych, R. Lupytsky, S. Minko, M. Stamm, *Macromolecules* **2005**, *38*, 501.
[35] S. Gupta, M. Agrawal, P. Uhlmann, F. Simon, U. Oertel, M. Stamm, *Macromolecules* **2008**, *41*, 8152.
[36] B. K. Kuila, M. Stamm, *J. Mater. Chem.* **2010**, *20*, 6086.
[37] G. Gattuso, S. A. Nepogodiev, J. F. Stoddart, *Chem. Rev.* **1998**, *98*, 1919.
[38] T. Shimomura, *J. Chem. Phys.* **2002**, *116*, 1753.
[39] M. Sowmiya, P. Purkayastha, A. K. Tiwari, S. S. Jaffer, S. K. Saha, *J. Photochem. Photobiol. A: Chem.* **2009**, *205*, 186.
[40] J. Kuang, J. Yuan, M. Zhou, W. Yuan, X. Sui, Z. Li, *Mater. Lett.* **2008**, *62*, 4078.
[41] Z. Xie, T. Lu, X. Chen, Y. Zheng, X. Jing, *J. Biomed. Mater. Res. A* **2009**, *88A*, 238.
[42] N. P. Lopes, K. E. Collins, I. C. S. F. Jardim, *J. Chromatogr.* **2003**, *987*, 77.
[43] L. Brown, T. Koerner, J. H. Horton, R. D. Oleschuk, *Lab Chip* **2006**, *6*, 66.
[44] D. J. T. Hill, A. K. Whittaker, in *Annual Reports on NMR Spectroscopy*, vol. *46* (Ed.: G. Webb), Academic Press, San Diego, **2002**, p. 1.
[45] W. Pyckhout-Hintzen, B. Müller, T. Springer, *J. Appl. Polym. Sci.* **1993**, *48*, 887.
[46] A. V. Kabanov, I. R. Nazarova, I. V. Astafieva, E. V. Batrakova, V. Y. Alakhov, A. A. Yaroslavov, V. A. Kabanov, *Macromolecules* **1995**, *28*, 2303.
[47] A. S. Lee, A. P. Gast, V. Bütün, S. P. Armes, *Macromolecules* **1999**, *32*, 4302.
[48] M. D. Abramoff, P. J. Magalhaes, S. J. Ram, *J. Biophotonics Int.* **2004**, *11*, 36.
[49] I. W. Hamley, *Block copolymers in solution: Fundamentals and applications*, Wiley, Hoboken, **2005**.
[50] J. A. Howarter, J. P. Youngblood, *Langmuir* **2006**, *22*, 11142.
[51] E. Metwalli, D. Haines, O. Becker, S. Conzone, C. G. Pantano, *J. Colloid Interface Sci.* **2006**, *298*, 825.
[52] A. Y. Fadeev, T. J. McCarthy, *Langmuir* **2000**, *16*, 7268.
[53] D. H. Dinh, L. Vellutini, B. Bennetau, C. Dejous, D. Rebiere, E. m. Pascal, D. Moynet, C. Belin, B. Desbat, C. Labrugere, J.-P. Pillot, *Langmuir* **2009**, *25*, 5526.
[54] S. Kawaguchi, G. Imai, J. Suzuki, A. Miyahara, T. Kitano, K. Ito, *Polymer* **1997**, *38*, 2885.
[55] L. Deschenes, M. Bousmina, A. M. Ritcey, *Langmuir* **2008**, *24*, 3699.
[56] R. A. Segalman, K. E. Schaefer, G. H. Fredrickson, E. J. Kramer, S. Magonov, *Macromolecules* **2003**, *36*, 4498.
[57] C. Yagüe, M. Moros, V. Grazú, M. Arruebo, J. Santamaría, *Chem. Eng. J.* **2008**, *137*, 45.
[58] D. J. Irvine, A. M. Mayes, S. K. Satija, J. G. Barker, S. J. Sofia-Allgor, L. G. Griffith, *J. Biomed. Mater. Res.* **1998**, *40*, 498.

Copyright © 2012 John Wiley & Sons, Ltd.

APPENDIX B

Preparation and evaluation of PEO-coated materials for a microchannel hemodialyzer

Keely Heintz, Karl F. Schilke, Joshua Snider, Woo-Kul Lee[a], Mitchell Truong, Matthew Coblyn, Goran Jovanovic, and Joseph McGuire[b]

School of Chemical, Biological and Environmental Engineering, Oregon State University, Corvallis, OR 97331

[a] Permanent address: Department of Chemical Engineering, Dankook University, 126 Jukjeun-dong, Suji-gu, Yongin-si, Gyeonggi-do, 448-701, Korea

[b] Corresponding author: joseph.mcguire@oregonstate.edu; 541-737-4600 (fax); 541-737-6306 (tel)

ABSTRACT

The marked increase in surface-to-volume ratio associated with microscale devices for hemodialysis leads to problems with hemocompatibility and blood flow distribution that are more challenging to manage than those encountered at the conventional scale. In this work stable surface modifications with pendant polyethylene oxide (PEO) chains were produced on polydimethylsiloxane (PDMS), polycarbonate microchannel and polyacrylonitrile membrane materials used in construction of microchannel hemodialyzer test articles. PEO layers were prepared by radiolytic grafting of PEO-polybutadiene-PEO (PEO-PB-PEO) triblock polymers to the material surfaces. Protein repulsion was evaluated by measurement of surface-bound enzyme activity following contact of uncoated and PEO-coated surfaces with β-galactosidase. Protein adsorption was decreased on PEO-coated polycarbonate and PDMS materials to about 20% of the level recorded on the uncoated materials. Neither the triblocks nor the irradiation process was observed to have any effect on protein interaction with the polyacrylonitrile membrane, or its permeability to urea. This approach holds promise as a means for *in situ* application of safe, efficacious coatings to microfluidic devices for blood processing that will ensure good hemocompatibility and blood flow distribution, with no adverse effects on mass transfer.

Keywords: PEO-polybutadiene-PEO triblock polymer; polyacrylonitrile membrane; polycarbonate; protein repulsion; urea permeability

Running Head: PEO-coated materials for a microchannel hemodialyzer

INTRODUCTION

An abundant literature describes the nonfouling (i.e. protein and cell repelling) mechanisms of material surfaces presenting pendant polymer chains, with particular emphasis having been placed on the function of pendant PEO [1-6]. However, despite clear evidence of the nonfouling character of PEO layers, clinical use of PEO-coated biomaterials is rare. Progress toward clinical application has historically been impeded by the lack of cost effective, non-invasive methods for preparation of stable, high density PEO layers on biomedical polymers.

Direct chemical modification of polymer materials used in biomedical devices with PEO is generally infeasible, due to the material chemistry and adverse effects on bulk material properties. Much research has thus focused on the use of PEO-containing block copolymers to produce nonfouling surfaces [2,7-11]. Pluronic® surfactants are triblock copolymers (PEO-PPO-PEO, where PPO = polypropylene oxide) that self-assemble onto hydrophobic materials from aqueous solutions. The PPO center block forms a strong hydrophobic association with the surface, while the hydrophilic PEO end chains remain freely mobile in the fluid [12]. Using this approach, a thick (10-20 nm) PEO brush layer is formed at the material surface, and effectively prevents the adsorption and adhesion of proteins, platelets, bacteria, and other cells [13,14]. However, triblock polymers that are immobilized only by hydrophobic association are subject to competitive elution from surfaces in the presence of whole blood. To overcome this limitation, glass and other metal oxides can be pretreated with vinyl-containing silanes, coated with triblocks, and then subjected to γ-irradiation. During irradiation, surface-bound free radicals are formed by absorption of radiation by the vinylic C=C bonds on the surface or through radiolytic formation of water-derived radicals. These free radicals attack the adsorbed PPO block, forming new covalent (permanent) bonds between the surface and polymer [3,9,15].

Polymeric materials, however, are not amenable to such chemical surface pretreatment. In this research we overcome this obstacle and avoid the need for pretreatment entirely, by using triblock copolymers that incorporate a vinyl group-rich polybutadiene center block to produce stable PEO coatings on the materials used in this work. Vinyl groups in the polybutadiene (PB) backbone will form radicals upon exposure to UV- or γ-irradiation under water[4,16,17], directly and permanently linking the triblocks to the otherwise unmodified biomaterial surface. This non-invasive approach avoids the use of toxic and expensive crosslinkers or harsh solvents that may alter the properties of the underlying material, and is directly applicable to most medical materials (e.g. arterial/venous accesses, blood tubing, polymeric devices, etc.).

Recently, our laboratory formed highly stable, protein-repellant PEO layers on medical grade Pellethane® and Tygon® polyurethanes by adsorption and γ-stabilization of PEO-PB-PEO triblocks[18]. The same triblocks were used in this research to coat microchannel and membrane materials, in support of design and development of a hemodialyzer based on engineered microscale flow features. Overall, our aim is to identify microfabrication and surface modification criteria for effective flow distribution and hemocompatibility within the device, while causing no adverse effects on mass transfer through the dialysis membrane. In this paper, the formation and characterization of pendant PEO layers is described, and layer function is evaluated in relation to protein repulsion of the coated microchannel materials. Finally, we discuss the impact of the triblock coatings on the transport of urea (a model uremic solute) through commercial flat-sheet polyacrylonitrile (PAN) hemodialysis membranes, both with and without a pre-applied polyethyleneimine (PEI) coating.

MATERIALS AND METHODS

Polymers and reagents

Polycarbonate (PC) sheets of ~500 µm thickness (McMaster-Carr, Santa Fe Springs, CA) were cut into samples of desired size, cleaned with ethanol and then dried with nitrogen[19]. Sylgard-184 polydimethylsiloxane (PDMS, Ellsworth Adhesives, Germantown, WI) was prepared by mixing silicone elastomer base and curing agent (10:1), poured into molds, degassed under vacuum for 45 min, and cured for 1 h at 75°C. Gambro AN69 and AN69-ST polyacrylonitrile (PAN) hemodialysis membranes (Home Dialysis Plus, Sunnyvale, CA), were cut into samples of desired size, and soaked in HPLC water for a minimum of 1 h to remove preservative glycerol. Hydroxyl-terminated polyethylene oxide-polybutadiene-polyethylene oxide (PEO-PB-PEO) triblock surfactants were purchased from the University of Minnesota Polymer Synthesis Facility (Minneapolis, MN), stored desiccated at -20°C under argon, and used without further purification. These triblocks have polybutadiene centerblocks (M_n = 620) with 73% vinyl side-groups (i.e. 1,2-addition product), and PEO side-chains of M_n = 2,845 (Figure 1). The polydispersity index of the triblock copolymers (by size-exclusion chromatography) was about 1.11.

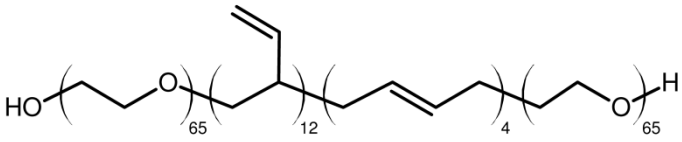

Figure 1: Approximate chemical structure of PEO-PB-PEO triblock copolymer surfactant used to produce PEO brush layers.

Fungal *ß*-galactosidase from *Aspergillus oryzae*, plasminogen-free human fibrinogen, and bovine serum albumin (BSA) were purchased from Sigma-Aldrich (St. Louis, MO), and used without further purification. All aqueous solutions were made with HPLC-grade water. All other reagents

and solvents were of ACS reagent grade or better, and used as received from commercial vendors.

Evaluation of the critical aggregation concentration (CAC) of PEO-PB-PEO triblocks

The CAC of the PEO-PB-PEO triblocks was determined by a pyrene fluorescence method[20,21]. Triblock solutions of various concentrations were prepared in water containing pyrene at a final concentration of 10^{-4} mg/mL. Solutions were covered to minimize light exposure and incubated at 35°C for about 24 h, after which the fluorescence intensity was measured with excitation and emission wavelengths of λ_{ex} = 338 nm and λ_{em} = 395 nm, respectively (FluoroLog 3, Horiba Scientific, Edison, NJ).

Coating of polymer surfaces with PEO-PB-PEO triblocks

Solutions of PEO-PB-PEO triblocks in water, with or without added salt (150, 300, or 500 mM NaCl), were prepared at selected triblock concentrations. Polymer samples (PC, PDMS, and PAN membrane) were individually covered with either triblock solution or triblock-free water, and incubated 12-24 h at 20°C, to allow self-assembly of the triblocks on the polymer surfaces. Exposure of triblock solutions to light was minimized by covering all solution containers with foil. The uncoated or triblock-coated samples were then γ-irradiated with a ^{60}Co source over 8 h to a total dose of 0.3 Mrad. After irradiation, the polymer samples were rinsed three times with 20 mM phosphate-citrate buffer at pH 4.5, to condition the surface for enzyme adsorption and remove any loosely held or unbound triblocks. In separate experiments, the stability of the γ-irradiated triblock layers was tested by rinsing vigorously for 1 h with 5% sodium dodecylsulfate (SDS) in 10 mM sodium phosphate with 150 mM NaCl, pH 7.4 (PBS).

Evaluation of protein repulsion by PEO layers

Polymer samples were incubated at 20 °C in phosphate-citrate buffer, in the presence or absence of 1 mg/mL ß-galactosidase, on a reciprocal shaker to allow for protein adsorption. After rinsing with enzyme-free phosphate-citrate buffer to remove any loosely held enzyme, nitrile O-rings were placed on the polymer samples, and filled with a solution of 1 mM *o*-nitrophenyl-*β*-D-galactopyranoside (*o*-NPG) in phosphate-citrate buffer. The O-rings provide a known, repeatable reaction volume and surface area in contact with the *o*-NPG substrate solution. After incubation at 37°C for 3 h, the substrate solution was carefully mixed and triplicate 80 µL samples taken. After addition of two volumes of 200 mM borate buffer (pH 9.8) to raise the sample pH[22], the relative amount of adsorbed ß-galactosidase was quantified by measurement of the resulting yellow *o*-nitrophenolate ion (*o*-NP^-) at 405 nm (Figure 2).

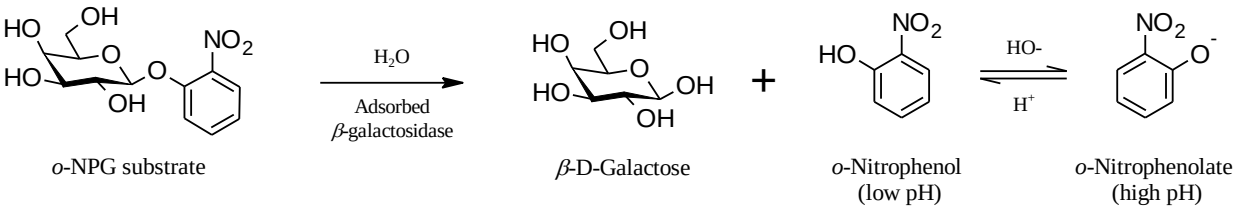

Figure 2: Hydrolysis of *o*-NPG substrate catalyzed by adsorbed ß-galactosidase enzyme.

Evaluation of urea permeability of treated membranes

The impact of the triblock coating procedure on the mass transfer performance of the AN69 and AN69-ST membranes was examined by comparing the transport of urea through treated and untreated membranes. For this purpose a stirred cell was built featuring two well-mixed 80 mL compartments on each side of a membrane sample, which was supported by PVC rubber gaskets (Figure 3). The exposed membrane area for mass transfer was 16 cm^2 in each case. Liquid from

the permeate compartment was pumped continuously to a 240 mL reservoir, and from that reservoir returned to the permeate compartment.

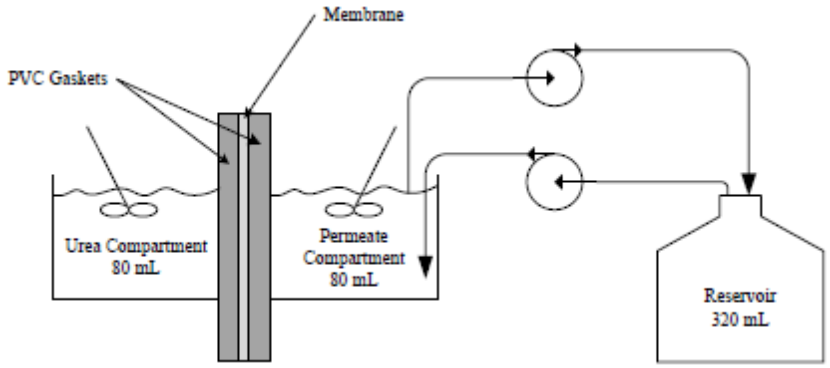

Figure 3. Schematic of stirred flow cell used for evaluation of urea transport.

An experiment began with the reservoir chamber containing PBS, while the urea chamber contained either (i) 0.3 mg/mL urea in PBS; (ii) 0.3 mg/mL urea in PBS with 5 mg/mL BSA, or (iii) 0.3 mg/mL urea in PBS with 1 or 2 mg/mL fibrinogen. Triplicate 200 µL samples were taken every 30 min for a period of 5 h, and urea concentration was measured by colorimetry (450 nm) after reaction with *o*-phthalaldehyde and primaquine bisphosphate[23] for 1 h at 37°C.

RESULTS

Evaluation of the critical aggregation concentration (CAC) of PEO-PB-PEO triblocks

The fluorescence intensity of pyrene in triblock solutions in water, when plotted vs. the log of the triblock concentration, exhibits two-region behavior which is consistent with the onset of micellization or aggregate formation above a critical concentration (Figure 4). Two linear regions were identified, and the triblock concentration at the intersection of these regions corresponds to the critical aggregation concentration (CAC). Within 95% confidence intervals (gray, $n = 3$), the CAC of PEO-PB-PEO triblocks at 25°C was 2.2 ± 0.3 mg/mL.

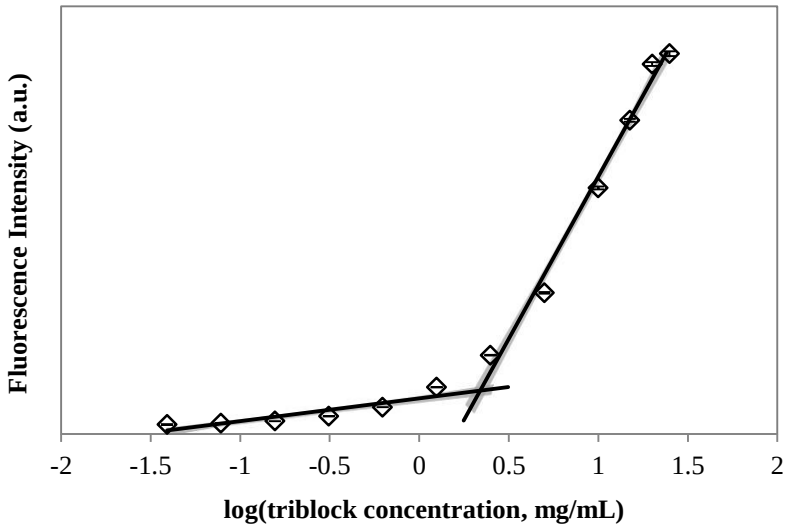

Figure 4: Pyrene fluorescence of PEO-PB-PEO triblocks in water. Error bars show the standard error of each concentration, gray shaded areas correspond to 95% confidence bands.

Characterization of PEO layer stability

ß-galactosidase enzyme activity (normalized to that of a bare, uncoated PC surface) was recorded on PEO-coated PC surfaces which had been coated from solutions of PEO-PB-PEO triblock at concentrations less than and greater than the CAC. The enzyme activity assay was performed on γ-stabilized as well as non-irradiated, coated polymer samples, which were rinsed in the presence or absence of SDS (or not rinsed at all), in advance of protein contact. The PEO layers prepared using triblocks at 1 mg/mL (Figure 5a) and 5 mg/mL (Figure 5b) showed almost no enzyme activity, indicating very good protein repulsion, if no rinse step preceded protein challenge (treatment "A"). Little difference was observed between the unstabilized and γ-irradiated coatings.

When rinsed with buffer in the absence of SDS (treatment "B"), however, the increased *ß*-galactosidase activity indicates that a significant portion of the triblocks were removed from the polycarbonate surface. This suggests that there remains a population of triblocks which are not covalently stabilized by the treatment with γ-irradiation. Finally, when rinsed vigorously with

SDS in advance of protein contact (treatment "C"), an even greater portion of the triblock was apparently removed from the polycarbonate surface which was not subjected to γ-irradiation. In contrast, the polycarbonate samples which were γ-irradiated and then rinsed with SDS were nearly indistinguishable from those which were rinsed with SDS-free buffer, indicating that the remaining triblocks are stably associated with the surface.

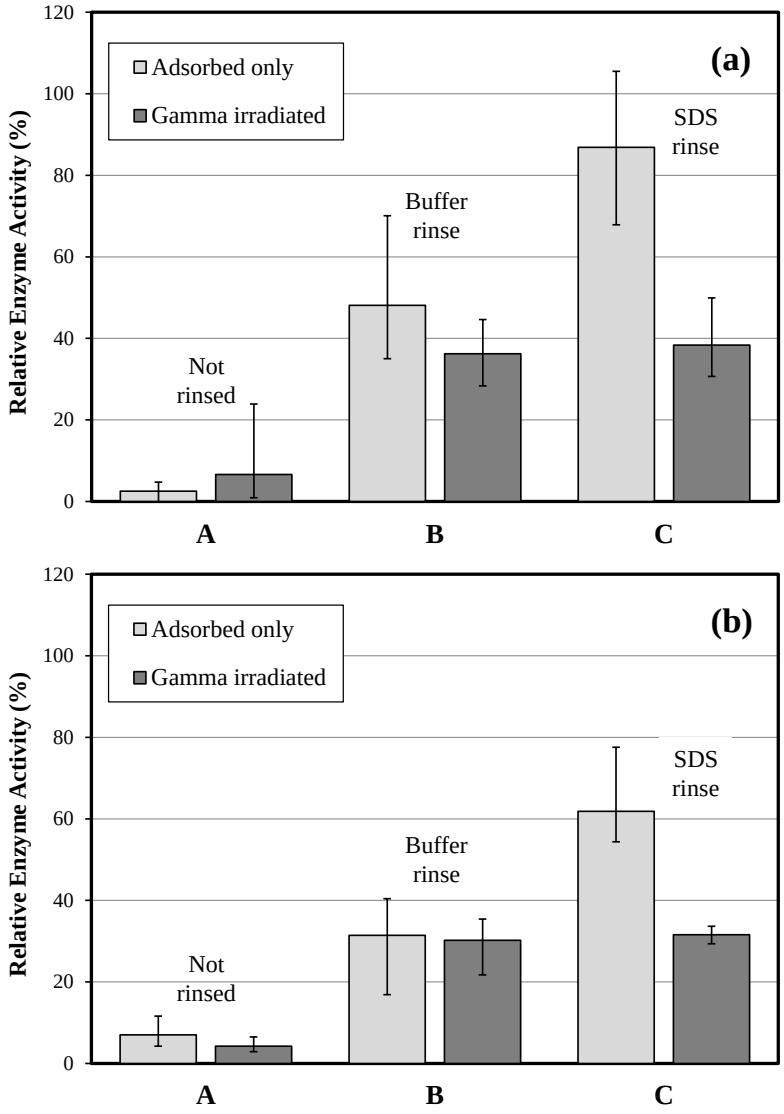

Figure 5: Average ß-galactosidase enzyme activity on polycarbonate coated from solutions of (a) 1 mg/mL, or (b) 5 mg/mL PEO-PB-PEO. After coating, with or without γ-irradiation, samples were not rinsed (A), rinsed three times per side with phosphate citrate buffer (B), or rinsed for one hour in PBS with SDS (C). Activity is normalized to the average enzyme activity of uncoated, bare PC surfaces (data not shown). Error bars indicate minimum/maximum values (n = 3).

Protein repulsion by PEO layers on polycarbonate and PDMS

The effect of γ-irradiation in the presence and absence of PEO-PB-PEO triblocks on ß-galactosidase adsorption to polycarbonate was also investigated. Adsorption of ß-galactosidase on polycarbonate is slightly reduced after γ-irradiation in water (Figure 6, treatment "B"). In contrast, irradiation with triblocks at concentrations from 1 to 10 mg/mL (treatments "C" to "E") greatly reduced the adsorption of enzyme. No obvious concentration dependence on protein repulsion was revealed in these tests, and hence surface coatings were prepared using a 1 mg/mL triblock solution for all subsequent tests.

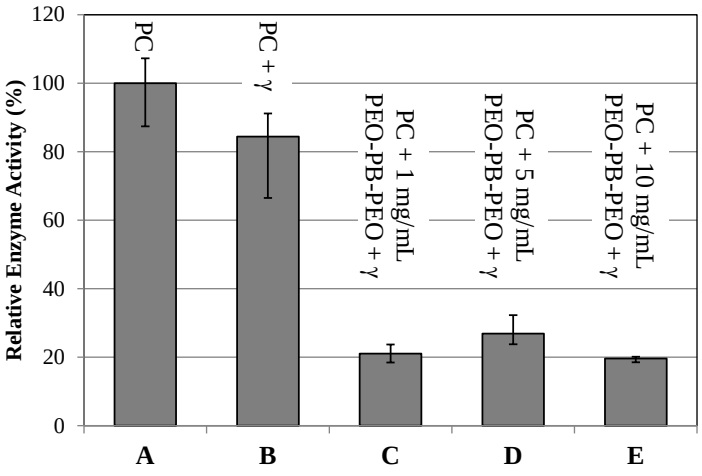

Figure 6: Average enzyme activity for ß-galactosidase adsorbed on bare PC (A), PC γ-irradiated in water (B), or on PC irradiated with 1, 5, or 10 mg/mL PEO-PB-PEO (C, D, and E). Error bars indicate minimum and maximum values (n = 3).

Similarly to polycarbonate, ß-galactosidase adsorption on PDMS is slightly reduced by γ-irradiation in water (Figure 7, treatment "B"). Enzyme adsorption is substantially reduced on PDMS which was γ-irradiated in the presence of 1 mg/mL PEO-PB-PEO (treatment "C"). In addition, protein adsorption on surfaces with γ-irradiated coatings ("C") was substantially lower than for coatings which were not stabilized by irradiation ("D").

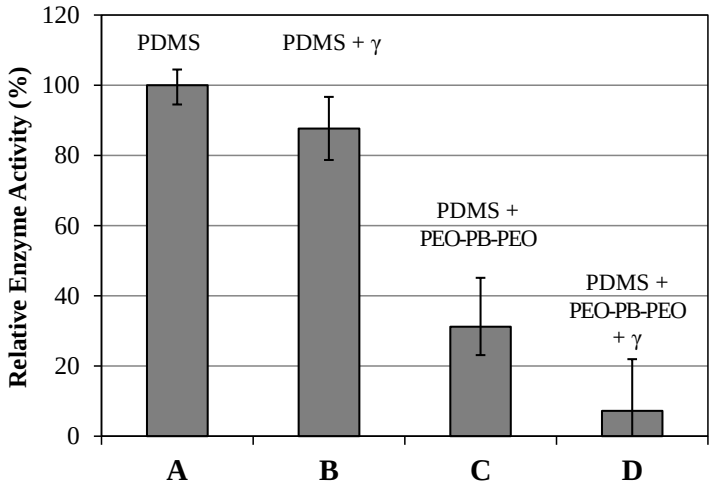

Figure 7: Average enzyme activity for ß-galactosidase adsorbed on bare PDMS (A), on PDMS γ-irradiated in water (B), PDMS irradiated with 1 mg/mL PEO-PB-PEO (C), or PDMS contacted with PEO-PB-PEO but not irradiated (D). Error bars indicate minimum and maximum values (n = 3).

The results in Figure 6 and Figure 7 are normalized to the enzyme activity exhibited by untreated polycarbonate and PDMS, respectively, and because of differences in the surface properties, they cannot be directly compared with each other. The average enzyme activity observed after exposure of untreated PDMS samples to β-galactosidase was only 34% that of the enzyme activity on untreated polycarbonate.

Effects of triblock coating on protein repulsion and mass transfer of PAN membranes

Samples of AN69-ST (PEI-coated PAN) membranes were exposed to β-galactosidase after irradiation in water and in the presence of 1 mg/mL PEO-PB-PEO triblocks. In both cases, the enzyme activity of the irradiated membrane samples was practically identical to the untreated AN69-ST membrane, indicating that there is no change in protein repulsion after treatment (data not shown).

Likewise, the rates of urea transport through untreated and γ-irradiated AN69 and AN69-ST polyacrylonitrile membranes were all very similar (Figure 8). Urea transport through the AN69-ST membrane was largely unaffected by the presence of PEO-PB-PEO triblocks. In addition, the

rates of urea transport across the triblock-coated and irradiated AN69-ST membranes were substantially unchanged by the presence of BSA and fibrinogen.

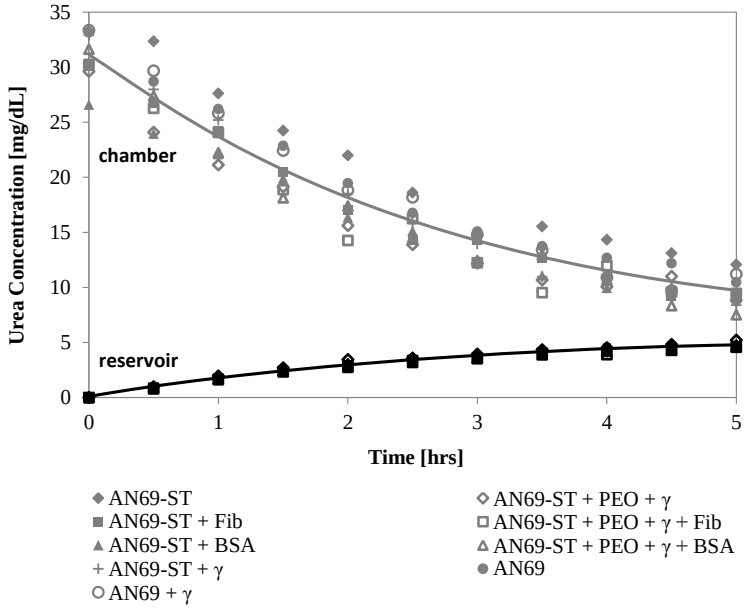

Figure 8: Comparison of urea transport kinetics through AN69 and AN69-ST membranes that were not irradiated (• and ♦) or γ-irradiated (○ and +) in water; (non-irradiated) AN69-ST membranes in the presence of BSA (▲) or fibrinogen (■); and AN69-ST membranes that were γ-irradiated in the presence of PEO-PB-PEO (◊), then placed in the presence of BSA (Δ) or fibrinogen (□). Solid lines are included to guide the eye. Data points represent averages of three samples at each time point.

DISCUSSION

Selection of coating conditions based on triblock CAC and PEO layer stability

During the self-assembly of triblock polymers at surfaces, the mechanism of adsorption as well as the adsorption kinetics depend on triblock solution concentration. At low concentration, the triblocks exist as individual surfactant molecules (unimers) and their adsorption may not cover the whole surface. At high concentration, however, the triblocks will form micelles or aggregates, and the PEO chains extending from these aggregates may inhibit the association between the hydrophobic center block and the surface[24]. Thus, it is fair to expect that adsorption of triblocks from a solution with a concentration slightly below the CAC (i.e. providing the

largest population of unimers) will give the most homogeneous coverage and highest grafting efficiency.

The CAC of the triblocks used here was determined to be about 2.2 mg/mL, using a pyrene fluorescence method (Figure 4). At triblock concentrations below the CAC, the pyrene molecules are surrounded by water and their fluorescence is largely quenched. When the CAC is reached, however, the triblocks begin to assemble into micelles or aggregates, and the hydrophobic pyrene molecules partition from the polar aqueous phase into the apolar interior of the micelles. The corresponding increase in fluorescence indicates the concentration at which aggregate formation begins[2,20,21] (i.e. the CAC).

For the purpose of further development of the coating procedure, we tested the protein repulsion of PEO layers prepared from triblock concentrations of 1, 5, and 10 mg/mL in water. Results of experiments represented in Figure 6 established that γ-stabilization followed by buffer rinse produced covalently stabilized PEO layers substantially free of any loosely held triblocks.

The presence of salt is generally expected to lower the CAC of triblock polymers containing PEO or other polyethers[25], and we anticipated that salt could be used to modulate the surface coverage of the PEO-PB-PEO during coating at a given triblock concentration. The enhanced surface coverage would presumably decrease the adsorption of proteins (e.g. *β*-galactosidase). However, no such effect was observed in tests with salt concentrations up to 500 mM NaCl (data not shown). It is possible that the ß-galactosidase assay may not be sensitive enough to detect the associated changes in PEO surface coverage.

Effect of PEO-PB-PEO on protein repulsion of PC and PDMS

While γ-irradiation in the presence of PEO-PB-PEO at 1 mg/mL produced only a modest reduction in the contact angle of water on polycarbonate (from 85° to 56°), the adsorption of ß-

galactosidase at coated polycarbonate surfaces was decreased by about 80% (Figure 5 and Figure 6). A similar trend was observed with PDMS (Figure 7), although the adsorption of ß-galactosidase was substantially reduced at even an unmodified PDMS surface when compared with PC. As the ß-galactosidase protein is smaller than fibrinogen (MW 105 vs. 340 Da), it is reasonable to assume that such PEO-PB-PEO layers would exhibit even better repulsion of fibrinogen. Tseng et al. recorded fibrinogen adsorption and platelet adhesion at surfaces coated with γ-stabilized PEO-PB-PEO triblocks, with PEO block molecular weights ranging from 350 to 5000 Da. They found that the pendant PEO chains were able to prevent platelet adhesion at all chain lengths studied, while platelet activation attributed to fibrinogen adsorption was suppressed only with 2 and 5 kDa chains[4]. The PEO blocks of the PEO-PB-PEO triblocks used in this study have a molecular weight around 2.8 kDa, suggesting that they fall into a size range that would minimize platelet activation. The decrease in protein adsorption, compared to the native surfaces, observed at γ-irradiated PDMS (Figure 6) and PC (Figure 7) is consistent with other reports[16]. The reduction in enzyme adsorption may be due to increased hydrophilicity of the surface caused by radical-based oxidation during irradiation[26-28]. However, these effects are expected to be short-lived due to relaxation of the polymer surface, particularly in the case of PDMS[29,30].

Effect of PEO-PB-PEO on protein repulsion of AN69-ST hemodialysis membrane

The AN69-ST membrane is coated by the manufacturer with a layer of highly cationic PEI, to provide a high affinity support for electrostatic immobilization of circulating heparin in advance of hemodialysis[31]. Because of the highly ionic and hydrophilic character of the membrane, it is likely that the triblock affinity for PEI is simply too low to create a protein-repulsive layer, and

hence the adsorption of β-galactosidase was unaffected by the presence of triblocks or irradiation (data not shown).

Effects on urea permeability of PEO-PB-PEO-coated membranes

Neither coating with triblocks nor γ-irradiation in water or triblock solution affected the urea transport through the AN69 membrane materials tested here. Concerning its application to a hemodialyzer based on microscale flow features, the results described above (good protein repulsion, and no effect on mass transfer) strongly suggest that the coating could be applied *in situ* to an assembled device, thus providing a steric barrier to protein adsorption on the polycarbonate microchannels without adversely affecting the dialysis membrane function. In addition, biomedical devices made from PC can be sterilized by γ-irradiation, potentially making it quite economical to stabilize the triblock coating by exposure to radiation.

Importance of coating properties to microchannel-based hemodialysis

Although biocompatibility is of course very important, in a microfluidic context the coating will also preempt problems with flow maldistribution (owing mainly to bubble retention). Because the microchannels and bubbles are of similar length scales, these issues cannot be managed as they would be at the conventional scale. Bubbles arise during normal setup and operation of any such microfluidic device, as well as from outgassing and nucleation within the device. Bubbles become lodged on surfaces within the microchannel array, where they obstruct flow or otherwise disrupt proper flow distribution. These effects not only decrease overall filtration performance, but can also lead to blood damage caused by the high shear zones created around bubbles, contact of blood proteins with the hydrophobic air-water interface, and (indirectly) through the high velocities needed to drive bubbles through the microchannels. Thus, a viable blood contact

surface coating in this context must not only provide a steric repulsive barrier without compromising mass transfer, but also help ensure minimal bubble retention within the device.

In addition to the importance of microchannel geometry and manifold design, surface energetics can play a major role in governing multiphase flow at the microscale. Higher pressure drops are required to enforce a given flow rate through microchannels in the presence of bubbles[32], where bubble adhesion to the walls is mediated by adsorbed molecules on the bubble surface[33,34]. We recently fabricated a number of single lamina (40 microchannel), single membrane test devices and completed a visual image analysis of flow maldistribution associated with the introduction of air bubbles into coated and uncoated microchannel arrays. Test articles coated as described above had significantly fewer channels obstructed by bubbles at a given fluid velocity. This is particularly important in this application, because operation at low velocities is at once more efficient for mass transfer and less damaging to the flowing blood. Fabrication, coating, and testing of those articles, with respect to the effect of air bubbles on flow distribution as well as fluid residence time distribution within these single lamina devices, will be described in a separate report.

ACKNOWLEDGMENTS

The authors thank Dr. Angelique White and Katie Watkins-Brandt for the use of the Fluorolog 3 spectrofluorometer. This work was supported in part by the National Institute of Biomedical Imaging and Bioengineering (NIBIB, grant no. R01 EB011567). The content is solely the responsibility of the authors and does not necessarily represent the official views of NIBIB or the National Institutes of Health.

REFERENCES

1. de Gennes PG. Polymers at an interface; a simplified view. Adv Colloid Interface Sci 1987;27(3-4):189-209.
2. McPherson T, Kidane A, Szleifer I, Park K. Prevention of protein adsorption by tethered poly(ethylene oxide) layers: Experiments and single-chain mean-field analysis. Langmuir 1998;14(1):176-186.
3. McPherson TB, Shim HS, Park K. Grafting of PEO to glass, nitinol, and pyrolytic carbon surfaces by γ irradiation. J Biomed Mater Res 1997;38(4):289-302.
4. Tseng Y-C, McPherson T, Yuan CS, Park K. Grafting of ethylene glycol-butadiene block copolymers onto dimethyl-dichlorosilane-coated glass by γ-irradiation. Biomaterials 1995;16(13):963-972.
5. Unsworth LD, Sheardown H, Brash JL. Polyethylene oxide surfaces of variable chain density by chemisorption of PEO-thiol on gold: Adsorption of proteins from plasma studied by radiolabelling and immunoblotting. Biomaterials 2005;26(30):5927-5933.
6. Unsworth LD, Sheardown H, Brash JL. Protein-resistant poly(ethylene oxide)-grafted surfaces: Chain density-dependent multiple mechanisms of action. Langmuir 2008;24(5):1924-1929.
7. Lee JH, Ju YM, Kim DM. Platelet adhesion onto segmented polyurethane film surfaces modified by addition and crosslinking of PEO-containing block copolymers. Biomaterials 2000;21(7):683-691.
8. Park JH, Cho YW, Kwon IC, Jeong SY, Bae YH. Assessment of PEO/PTMO multiblock copolymer/segmented polyurethane blends as coating materials for urinary catheters: In vitro bacterial adhesion and encrustation behavior. Biomaterials 2002;23(19):3991-4000.
9. Park K, Shim Hong S, Dewanjee Mrinal K, Eigler Neal L. In vitro and in vivo studies of PEO-grafted blood-contacting cardiovascular prostheses. J Biomater Sci Polym Ed 2000;11(11):1121-1134.
10. Tai Y-C, Joshi P, McGuire J, Neff JA. Nisin adsorption to hydrophobic surfaces coated with the PEO–PPO–PEO triblock surfactant pluronic® f108. J Colloid Interface Sci 2008;322(1):112-118.
11. Tai Y-C, McGuire J, Neff JA. Nisin antimicrobial activity and structural characteristics at hydrophobic surfaces coated with the PEO–PPO–PEO triblock surfactant pluronic® f108. J Colloid Interface Sci 2008;322(1):104-111.
12. Li J-t, Carlsson J, Huang S-C, Caldwell Karin D. Adsorption of poly(ethylene oxide)-containing block copolymers. Hydrophilic polymers: American Chemical Society; 1996. p 61-78.
13. Neff JA, Caldwell KD, Tresco PA. A novel method for surface modification to promote cell attachment to hydrophobic substrates. J Biomed Mater Res 1998;40(4):511-519.
14. Neff JA, Tresco PA, Caldwell KD. Surface modification for controlled studies of cell–ligand interactions. Biomaterials 1999;20(23-24):2377-2393.
15. Ryder MP, Schilke KF, Auxier JA, McGuire J, Neff JA. Nisin adsorption to polyethylene oxide layers and its resistance to elution in the presence of fibrinogen. J Colloid Interface Sci 2010;350(1):194-199.
16. Kidane A, McPherson T, Shim HS, Park K. Surface modification of polyethylene terephthalate using PEO-polybutadiene-PEO triblock copolymers. Colloids Surf B Biointerfaces 2000;18(3-4):347-353.

17. Schilke KF, Snider JL, Jansen LE, McGuire J. Direct imaging of the surface distribution of immobilized cleavable polyethylene oxide-polybutadiene-polyethylene oxide triblock surfactants by atomic force microscopy. Surf Interface Anal 2013;45(4):859-864.
18. Schilke KF, McGuire J. Detection of nisin and fibrinogen adsorption on poly(ethylene oxide) coated polyurethane surfaces by time-of-flight secondary ion mass spectrometry (TOF-SIMS). J Colloid Interface Sci 2011;358(1):14-24.
19. Tsuzuki Y, Oikubo Y, Matsuura Y, Itatani K, Koda S. Vacuum ultraviolet irradiation on siliceous coatings on polycarbonate substrates. J Sol-Gel Sci Technol 2008;47(2):131-139.
20. Croy SR, Kwon GS. Polysorbate 80 and Cremophor EL micelles deaggregate and solubilize nystatin at the core–corona interface. J Pharm Sci 2005;94(11):2345-2354.
21. Goddard ED, Turro NJ, Kuo PL, Ananthapadmanabhan KP. Fluorescence probes for critical micelle concentration determination. Langmuir 1985;1(3):352-355.
22. Schilke KF, Wilson KL, Cantrell T, Corti G, McIlroy DN, Kelly C. A novel enzymatic microreactor with *Aspergillus oryzae* β-galactosidase immobilized on silicon dioxide nanosprings. Biotechnol Prog 2010;26(6):1597-1605.
23. Huang S-G, Kwan P, Llinas M, Olszewski KL, Zawada RJX. Quantitative determination of urea concentrations in cell culture medium. Biochem Cell Biol 2009;87(3):541+.
24. Leermakers FAM, Gast AP. Block copolymer adsorption studied by dynamic scanning angle reflectometry. Macromolecules 1991;24(3):718-730.
25. Patel K, Bharatiya B, Kadam Y, Bahadur P. Micellization and clouding behavior of EO–PO block copolymer in aqueous salt solutions. J Surfact Deterg 2010;13(1):89-95.
26. Wong I, Ho C-M. Surface molecular property modifications for poly(dimethylsiloxane) (PDMS) based microfluidic devices. Microfluid Nanofluid 2009;7(3):291-306.
27. Alexander P, Charlesby A. Effect of X-rays and γ-rays on synthetic polymers in aqueous solution. Journal of Polymer Science 1957;23(103):355-375.
28. Denaro AR, Jayson GG. Fundamentals of radiation chemistry. London: Butterworth 1972.
29. Ozdemir M, Yurteri CU, Sadikoglu H. Physical polymer surface modification methods and applications in food packaging polymers. Crit Rev Food Sci Nutr 1999;39(5):457-477.
30. Rangel E, Gadioli G, Cruz N. Investigations on the stability of plasma modified silicone surfaces. Plasmas Polym 2004;9(1):35-48.
31. Richtrova P, Opatrny K, Vit L, Sefrna F, Perlik R. The AN69 ST haemodialysis membrane under conditions of two different extracorporeal circuit rinse protocols—a comparison of thrombogenicity parameters. Nephrology Dialysis Transplantation 2007;22(10):2978-2984.
32. Cubaud T, Ho C-M. Transport of bubbles in square microchannels. Phys Fluids 2004;16(12):4575-4585.
33. Stephen JH, Wong ZZ, Bull JL. Perfluorocarbon bubble occlusion mechanisms within an in vitro microfluidic model of the microcirculation. ASAIO J 2006;52(4):493.
34. Wong ZZ, Stephen J, Bull J. Effect of bubbles on cell viability in a circular-lumen endothelialized microvascular model. ASAIO J 2006;52(4):494.